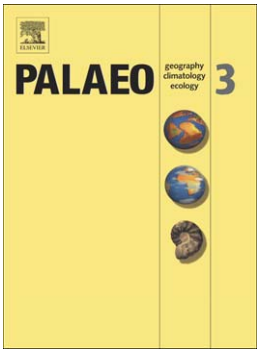

Interpreting vegetation change in tropical arid ecosystems from sediment molecular fossils and their stable isotope compositions: A baseline study from the Pilbara region of northwest Australia

Alexandra Rouillard, Paul F. Greenwood, Kliti Grice, Grzegorz Skrzypek, Shawan Dogramaci, Chris Turney, Pauline F. Grierson

PII: S0031-0182(16)30278-4
DOI: doi: 10.1016/j.palaeo.2016.07.023
Reference: PALAEO 7914

To appear in: *Palaeogeography, Palaeoclimatology, Palaeoecology*

Received date: 6 March 2016
Revised date: 8 July 2016
Accepted date: 19 July 2016

Please cite this article as: Rouillard, Alexandra, Greenwood, Paul F., Grice, Kliti, Skrzypek, Grzegorz, Dogramaci, Shawan, Turney, Chris, Grierson, Pauline F., Interpreting vegetation change in tropical arid ecosystems from sediment molecular fossils and their stable isotope compositions: A baseline study from the Pilbara region of northwest Australia, *Palaeogeography, Palaeoclimatology, Palaeoecology* (2016), doi: 10.1016/j.palaeo.2016.07.023

ARTICLE TYPE

Research Paper

TITLE

Interpreting vegetation change in tropical arid ecosystems from sediment molecular fossils and their stable isotope compositions: A baseline study from the Pilbara region of northwest Australia

AUTHORS

Alexandra Rouillard[11*], Paul F Greenwood[1-3], Kliti Grice[3], Grzegorz Skrzypek[1], Shawan Dogramaci[4], Chris Turney[5], Pauline F Grierson[1]

1. West Australian Biogeochemistry Centre and Ecosystems Research Group, School of Plant Biology, The University of Western Australia (UWA), Crawley WA, Australia.

2. Centre for Exploration Targeting, School of Earth and Environment, UWA.

3. Western Australia Organic and Isotope Geochemistry Centre; and John de Laeter Centre, The Institute for Geoscience Research, Department of Chemistry, Curtin University, Perth WA, Australia

4. Rio Tinto Iron Ore, Perth WA, Australia.

5. Climate Change Research Centre, University of NSW, Sydney NSW, Australia.

* Corresponding author: e-mail: alexandra.rouillard@snm.ku.dk; alexandrarouillard@yahoo.ca

[1] Present address: Centre for GeoGenetics, The Natural History Museum of Denmark, Øster Voldgade 5-7, 1350 Copenhagen K, Denmark

KEY WORDS

Biomarkers; CSIA $\delta^{13}C$; *n*-alkanes; organic matter; Pilbara; *Triodia*

ABSTRACT

Detection of source diagnostic molecular fossils (biomarkers) within sediments can provide valuable insights into the vegetation and climates of past environments. However, hot and arid regions offer particularly challenging interpretive frameworks for reconstructions because baseline data are scarce, organic matter is generally very low and in the inland tropics in particular, sediments are also often subject to flooding and drought. Here, we investigated whether biomarkers and compound-specific $\delta^{13}C$ values could be extracted from a late Holocene sediment record from the Fortescue Marsh (Pilbara, northwest Australia) to allow interpretation of past catchment vegetation and hydroclimate. The low total carbon (TC) content (<1.4 %) was a major challenge for the molecular analyses over the ~2000 years old sequence. Nevertheless, they revealed that the dominant hydrocarbon features (e.g., long chain *n*-alkanes) indicative of terrestrial plants (e.g., C_4 grasses; riparian and other C_3 plants) encompassed the last ~1300 yrs and that low abundance of products from aquatic sources (e.g., *n*-C_{17}) were detected in the uppermost sediments only when permanently inundated conditions prevailed (recent decades). Similarly, the lower $\delta^{13}C$ values (i.e., a difference of -2.3 ‰) of long chain *n*-alkanes in upper sediments reflected a vegetation response to the emergence of wetter conditions through the late Holocene in the region. Based on the diverging dominant source contributions obtained from the molecular distributions and arid based Bayesian mixing model ($\delta^{13}C$ of *n*-$C_{27\text{-}33}$ alkanes) results, less arid conditions may have favoured the input of ^{13}C depleted *n*-alkanes from the *Eucalyptus* (C_3) dominant riparian vegetation. The deepest sediments (<CE 700) however, had a TC content of <0.4 %, and no organic compounds were detected, consistent with local and regional records of hyperarid conditions. These results demonstrate that *n*-alkanes can provide a molecular and stable isotopic fingerprint of important - and perhaps underappreciated - ecological processes in modern tropical arid environments for future paleoclimate investigations.

ABBREVIATIONS

CE Common Era

CPI Carbon preference index

CSIA Compound-specific stable isotope analysis

GC-MS Gas chromatography-Mass spectrometry

IRMS Isotope ratio mass spectrometry

OM Organic matter

TC Total carbon

1. INTRODUCTION

Lake sediment records can extend temporal scales of hydrologic reconstruction to millennial and longer time frames. For example, periods of drought can be reconstructed from changes in lake level and salinity using microfossil assemblages (e.g., diatoms) and geochemical or physical parameters of the sediment (e.g., Wolff et al. 2011; Barr et al. 2014). These paleolimnological methods have most commonly been applied to closed-basin lakes in arid or semiarid landscapes, in which changes in lake level and salinity are closely related to shifts in hydrologic balance (e.g., Stager et al. 2013). However, deep or permanent lakes are often lacking in many arid environments, resulting in limited applicability of many proxies due to preservation issues, notably for reconstructing inputs of organic matter to lakes that can reflect hydroclimate conditions. Organic geochemical studies of depositional environments have provided molecular evidence (biomarkers) of changing hydrology under various climates, including from the studies of lakes (Leng and Henderson 2013; Sun et al. 2013; Atahan et al., 2015), marine settings (e.g., Castañeda et al. 2009b; Dubois et al. 2014; Pagès et al. 2014), and coastal salt-marshes and lagoons (e.g.,

Volkman et al. 2007; McKirdy et al. 2010; Tulipani et al., 2014). The sedimentary distribution of biomarkers and their stable carbon and hydrogen isotope compositions (i.e., $\delta^{13}C$ and $\delta^{2}H$ at compound specific level) have been widely used to investigate physiological or ecological community responses to shifts in lake salinity and water source (Romero-Viana et al. 2012; Sachse et al. 2012; van Soelen et al. 2013). Variation in the $\delta^{13}C$ values of specific compounds, e.g., long chain *n*-alkanes representative of terrestrial vegetation, have also indirectly helped resolve past hydrological changes via their sensitivity to moisture availability in the catchment, drought stress or vegetation shifts (Castañeda et al. 2007; 2009a; Kristen et al. 2010; Tipple and Pagani 2010; Sun et al. 2013). Consequently, using biomarkers and their stable isotopes ratios to establish paleoenvironmental records for still underrepresented regions is of great interest.

Tropical arid ecosystems have proved especially challenging to paleolimnology and organic geochemical characterisation of sediments. These regions experience high seasonal and inter-annual hydroclimatic variability, typified by periods of prolonged droughts interspersed with occasional intense flooding (e.g., Rouillard et al. 2015; van Etten 2009). First, a general lack of water, which is often coupled with low nutrient availability, severely limits biological production and in turn the deposition of organic matter (OM) to sediments (e.g, Huxman et al. 2004; Snyder and Tartowski 2006; Collins et al. 2008; McIntyre et al. 2009a, b). In Australian soils of tropical (i.e., hot) arid environments in particular, the preservation of OM is further compromised by major biological reworking by termites and other fauna (e.g., Holt et al. 1987; Chen et al. 2003; Austin et al. 2004) and the high frequency of fires which can accelerate the loss of organic volatiles that might otherwise form terrestrial detritus (Ford et al. 2007). Intense episodic flooding can lead to increased mobilisation and dislocation of OM from the catchment to lakes followed by pulses of high organic production in the catchment and aquatic network, resulting in non-linear OM availability and deposition patterns (Battin et al. 2008; Reid et al. 2011; Puttock et al. 2012).

Shallow lakes mean that prolonged drought further exposes dried sediment to changing redox conditions and deflation, which can also cause hiatus of organic sedimentary records in many regions of the world (Verschuren et al. 1999; Bessems et al. 2008; Argus et al. 2014, 2015). Given these challenges, there have been few attempts to characterise such sediments in northwest Australia, a region where very limited knowledge of the Holocene environmental history is available to understand long-term ecosystem processes and resilience to ongoing climate change (Gergis et al. 2014).

Plant molecular δ^2H signals are normally considered indicative of the isotope ratio of source water and associated hydrology (Tipple and Pagani 2010; Romero-Viana et al. 2012; Sachse et al. 2012; van Soelen et al. 2013). However, the large evaporative shifts in lake volumes in arid and semi-arid regions generally result in salinity fluctuations that in turn affect the δ^2H fractionation between organisms and their source water (Sachse and Sachs 2008). In addition, plants make physiological adjustments to both changing water availability and salinity, which can also result in further fractionation (Zhou et al. 2011; Sachse et al. 2012), making plant molecular δ^2H less reliable than in more temperate or non-saline ecosystems (e.g., Duan et al., 2014). Consequently, plant molecular δ^{13}C compositions of sediments, particularly of *n*-alkanes, may be more suitable for hot arid environments.

The composition and distribution of plant communities in arid ecosystems is largely driven by the availability of water as well as other flooding or waterlogging-related conditions, such as soil redox, salinity, substrate and nutrient availability and the accumulation of toxic ions (Schwinning et al. 2004; Reid et al. 2011; Argus et al. 2014). Different hydrological regimes will favour plants of specific functional types (e.g., C_3 versus C_4 photosynthetic pathways, which are readily distinguished by their δ^{13}C signatures) and tolerance to drought, waterlogging or salinity (Huxman

et al. 2004; Snyder and Tartowski 2006). Prolonged aridity can thus progressively impact vegetation assemblages at the generation level over long timescales, generally favouring C_4 grasses across catchments and chenopods (often a mix of CAM, C_4 and C_3 species) in saline wetland areas (Sage et al. 2011). The ^{13}C enrichment of C_3 plant tissue can also be driven by water stress within a matter of minutes (Cernusak et al. 2013). The dynamics of plant water stress over periods of decades to centuries may also be recorded in the wood chemistry of trees (e.g., Cullen et al. 2008; Qin et al. 2015) or at the ecosystem level in soils and lake sediment (Krull et al. 2005, 2006; Diefendorf et al. 2011; Codron et al. 2013). Plants in arid environments also produce relatively high amounts of cuticular waxes as a protection against high ultraviolet light and water loss; cuticular waxes may thus represent more promising molecular targets of organic lean dryland sediments (Hoffmann et al. 2013).

Cuticular-derived *n*-alkanes (Eglinton and Hamilton 1967) are typically some of the more abundant products from the organic sediments of lakes (Schmidt et al. 2011), so are attractive analytes for compound specific isotopic analysis (CSIA). Characterisation of the molecular and stable isotopic abundances of *n*-alkanes has become an important paleoecological strategy to assess changes in hydrological status at catchment and continent scales (Castañeda and Schouten 2011; Sachse et al. 2012; Leng and Henderson 2013; Dubois et al. 2014). In recent years, the $\delta^{13}C$ values of *n*-alkanes in sediments have unlocked a wealth of paleoenvironmental information from regions and sites that had previously been difficult, including assessment of historical change in catchment land-use, eutrophication studies and shifts in vegetation composition in response to climate (e.g., Castañeda and Schouten 2011; Fang et al. 2014). However, as with other relatively new molecular tools in paleolimnology, our capacity to make inferences of paleo-flora from biomarkers is limited by uncertainties in source, transportation and preservation of OM from senescing plants (Birks and Birks 2016). A first step is to improve the baseline of available biomarker datasets and their

stable isotopic compositions from arid zone sediments with independently described paleoenvironmental histories.

Broadly, our study investigated the potential of organic molecular fossils and $\delta^{13}C$ values of plant waxes of lake sediments for reconstructing catchment vegetation history and hydroclimatic change in the arid subtropical Pilbara region of inland northwest Australia. Previously, we established centennial and millennial flood records for the Pilbara based on historical records as well as physical and geochemical analyses of sediments at the Fortescue Marsh (Rouillard et al. 2015; Rouillard et al. 2016). Here, we used a replicate core of this sediment sequence to determine if: i) organic geochemical information can be extracted to identify the major sources of sedimentary OM; ii) $\delta^{13}C$ values of individual organic molecules can be measured and related to the major vegetation types in the catchment (C_3 and C_4); and iii) the molecular and $\delta^{13}C$ distribution from the sedimentary sequence can be related to regional changes in hydrology through the late Holocene. Our analysis is considered within an interpretive framework that accounts for the specificities and challenges of extracting palaeoclimate information from organic geochemical indicators in sediments developed in tropical arid ecosystems.

2. METHODS

2.1 Study site

The study region and sampling is described in detail in Rouillard et al. (2016 in review). Briefly, replicated ~60-cm sediment cores (FOR106C2 and FOR106C3) were obtained from the deepest section of the 14 Mile Pool (22.6˚S, 119.9˚E) of the Fortescue Marsh in the arid Pilbara region of northwest Australia (Fig. 1). The pool is the most perennial water feature of the Fortescue Marsh, which acts as a terminal lake for the Upper Fortescue River catchment (31,000 km^2) (Skrzypek et. al. 2013). The Pilbara experiences highly episodic large hydrological events with high inter-annual

variability, i.e., creeks and rivers are generally dry with seasonal floods commonly occurring during the austral summer contributing brief periods of high flow (www.water.wa.gov.au). Evaporation is high in the eastern Pilbara (~2800–3200 $mm \cdot yr^{-1}$) and greatly exceeds average rainfall (290 $mm \cdot yr^{-1}$; www.bom.gov.au/climate/data). Flooding, drought and fire are the dominant and naturally occurring ecological disturbances in the region (McKenzie et al. 2009); variability in the seasonal and inter-annual hydrological cycle is extreme (Kennard et al. 2010; Rouillard et al. 2015) and likely influences the fire regime through feedback interactions (e.g., O'Donnell et al. 2011).

Vegetation across the hills and broad plains of the wider catchment is mainly shrub-steppe, dominated by C_4 grasses, especially spinifex (*Triodia* spp.) grasses and *Acacia* trees and shrubs (C_3). More permanent watercourses, including 14 Mile Pool, maintain a riparian fringe dominated by the trees *Eucalyptus camaldulensis* and *E. victrix* (C_3) (Fig. 1b, d; Beard 1975). Buffel grass (*Cenchrus ciliaris*—C_4) is an invasive perennial grass introduced in the 1920s that was also aerial seeded across the catchment in the 1960s to provide higher quality feed for cattle and sheep grazing; this grass is abundant in the floodplains of sections of the Upper Fortescue River (McKenzie et al. 2009). The Marsh downstream from 14 Mile Pool is dominated by chenopod shrubs, primarily *Tecticornia* species (Beard 1975) that have been attributed both C_3 and C_4 pathways (Carolin et al. 1982; Voznesenskaya et al. 2008; Moir-Barnetson 2014).

2.2 Analyses

2.2.1 Abundance and bulk stable isotopic values of total and organic sedimentary carbon

As per reported in Rouillard et al. (2016), relative abundance (%) and stable isotope composition (‰) of the sediment total C, organic C and total N were determined for every other interval (1 cm) of core FOR106C3 using a Thermo Flush Elemental Analyser coupled with a Delta V Plus Isotope Ratio Mass Spectrometer (Thermo Fisher Scientific, Bremen, Germany). Stable isotope results are

reported in permil (‰) after multi-point normalisation to international Vienna Pee Dee Belemnite standard (VPDB) scale using international reference materials NBS19, USGS24, NBS30, LSVEC (Skrzypek 2013), with combined analytical uncertainty <0.10 ‰. All samples were freeze-dried, ground using mortar and pestle and homogenised prior to analyses. To isolate the organic fraction, approximately 100–150 mg of ground sample was treated with 4 % HCl at room temperature overnight to remove carbonates prior to analysis. Acid pre-treatment for the removal of inorganic carbon (IC) can lead to biases beyond instrumental precision when measuring very low C abundance and corresponding $\delta^{13}C$ values (e.g., 4 ‰; Brodie et al. 2011), as is the case with the present low C content Pilbara sediments (Table 2). The total C and $\delta^{13}C$ results are therefore reported for total C without any acid pre-treatement i.e., without prior removal of inorganic C in the sediments.

2.2.2 Extraction and isolation of lipids

The sediment record of Fortescue Marsh at 14 Mile Pool comprises four distinct stratigraphic periods, together spanning several millennia of the marsh's environmental history (Rouillard et al. 2016). Replicate core FOR106C2 was separated into four sections each corresponding to one of the four periods, which were then each ground using mortar and pestle, homogenised and analysed for their molecular and stable carbon isotopic composition. Briefly, the sections and ages of the four periods we investigated and described in Rouillard et al. (2016) corresponded to Period 1 (P1; 1–19 cm, CE 1990–2012); Period 2 (P2; 19–40 cm, CE 1600–1990); Period 3 (P3; 40–49 cm, CE 700–1600) and 4 (P4; 49–61 cm, CE <100–700). Several dating methods (^{210}Pb, ^{137}Cs and ^{14}C) have coherently estimated the age of the record to encompass the last ~2000 years. Details of the dating procedures for the sediment record based on both replicates (FOR106C2 and FOR106C3) and hydrological interpretations based on the analysis of lithology, moisture content, particle size, microfossils, total C and N content and total stable isotope compositions ($\delta^{13}C$ and $\delta^{15}N$) on

replicate core FOR106C3 exclusively have been previously reported (Rouillard et al. 2016). To summarise the hydrological interpretations, near perennial aquatic conditions were inferred for P1; P2 sediments reflected a relatively drier and highly variable environment than P1 with episodic extreme flood disturbance; P3 and P4 both reflected generally more arid conditions than P1 and P2 and low energy hydrologies; conditions from the base of the record in P4 were likely hyperarid until relatively less arid conditions and more regular flooding established during P3 from ~CE 700 (Rouillard et al. 2016). Unfortunately, concentrations of pollen grains in the sequence were very low and high levels of deterioration were evident, likely reflecting the rewetting and subsequent drying of the sediment cracking clays (Cushing, 1967; Lowe, 1982). Therefore, pollen could not be used as a reliable indicator of past vegetation at this site (Rouillard et al. 2016).

The four samples (~20 g) from the FOR106C2 core were separately extracted in a Soxhlet apparatus using a mixture of dichloromethane (DCM) and methanol (90:10, v/v) for 48-hr. Elemental sulfur was removed through the extraction by the prior addition of activated copper turnings to the sample (Blumer 1957). The total solvent-extracted bitumen was separated by small column chromatography (activated silica stationary phase 150˚C, 8h; 4 cm Pasteur pipette) into saturate, aromatic and polar hydrocarbon fractions by successive elution with 2 mL *n*-hexane, 2 mL *n*-hexane:DCM (3:1) and 2 mL DCM:methanol (1:1) (Pagès et al. 2015). Fraction yields were quantified but with relatively high uncertainty because of the very low masses extracted (total extractable fraction <160 $\mu g \cdot g^{-1}$ dry sediment).

2.2.3 Gas chromatography - mass spectrometry (GC-MS) analysis of hydrocarbon fractions

GC-MS of the aliphatic and aromatic hydrocarbon fractions was conducted with an Agilent 6890 GC interfaced to a 5973 mass selective detector (MSD). The GC was fitted with a 60-m capillary column (HP 5MS, cross-linked 5 % phenyl 95 % methyl-polysiloxane, 0.25 mm i.d., 0.25 µm film

thickness), used He carrier gas (1.1 mL·min^{-1}) and analyses were conducted in pulsed splitless mode with the injector at 280˚C. Full scan (*m/z* 50–550) 70 eV mass spectra were acquired, with product assignments based on GC retention time or mass spectral correlation with the Wiley275 MS library, other laboratory standards or published data. Peak areas in the total ion chromatogram (TIC) were used for quantification, except for steroids and terpenoids whose peak areas were measured from *m/z* 217 and *m/z* 191 fragmentograms, respectively. Only products detected at > 1 % the total TIC or fragmentogram signals were used for quantification.

The P_{aq} index was calculated for each sediment period. P_{aq} is defined as:

$$(n\text{-}C_{23} + n\text{-}C_{25})/(n\text{-}C_{23} + n\text{-}C_{25} + n\text{-}C_{29} + n\text{-}C_{31})$$

and has been used previously as a proxy for the relative contributions of algal, macrophytic and terrestrial inputs in lacustrine environments (Ficken et al. 2000). In individual plants, P_{aq} values of >0.4 are consistent with mainly algal input; 0.1–0.4 indicates a mainly macrophytic source and <0.1 implies a mainly terrestrial origin.

2.2.4 Compound-specific δ^{13}C analyses

Compound-specific stable carbon isotope compositions were measured with an Agilent 6890 GC coupled with a Micromass IsoPrime2 isotope ratio mass spectrometer (IRMS). The GC instrument was fitted with a 60 m length, 0.25 mm i.d., 0.25 µm thick DB-1 phase column and analyses were conducted in pulsed splitless mode following setup as in Pagès et al. (2015). Stable carbon isotope compositions (‰), determined by integration of the m/z 44, 45 and 46 ion currents of the CO_2 peaks from each compound, were reported in the delta notation (δ^{13}C) all reported values are averages of at least triplicate analyses (standard deviation ≤0.2 ‰). The precision and accuracy of the isotopic measurements were maintained by multi-point normalisation using the linear regression slope and intercept obtained from frequent measurements (*n*=38; average standard deviation = 0.2 ‰) of an in-house standard mixture of *n*-alkanes (*n*-$C_{14,}$ -$C_{17,}$ -$C_{19,}$ and -C_{25}) of

known isotopic composition (respectively: -30.99, -29.72, -32.12, -31.94 ‰). Raw $\delta^{13}C$ values were recalculated to VPDB scale using multipoint normalisation based on an in-house standard mixture of four *n*-alkanes (*n*-C_{14}, -C_{17}, -C_{19}, and -C_{25}) of known isotopic composition (respectively: -30.99, -29.72, -32.12, -31.94 ‰ VPDB). Analytical precision of the stable isotope measurements were monitored by frequent measurements of laboratory standards (*n*=38), including the additional *n*-C_{11}, *n*-C_{13}, and *n*-C_{18} (respectively: -26.0; -29.3; -30.6 ‰ VPDB), during samples analyses and it was ≤0.2 ‰ (one standard deviation).

2.2.5 Mixing model to determine sources of n-*alkanes*

Probability estimates of the proportional contribution of terrestrial C_3 versus C_4 arid plants to the $\delta^{13}C$ values of the long-chain odd *n*-alkanes (*n*-C_{27} to *n*-C_{33}) were obtained using the Bayesian isotopic mixing model of the SIAR package (Parnell et al. 2010) in R v. 3.1.1 (MCMC = 30000). Two source end-members in the mixing model were based on a subset of leaf wax $\delta^{13}C$ values from C_3 and C_4 plants exclusively from arid regions and with taxonomic relevance to the Upper Fortescue River catchment (summarised in Table 1) to account foliar $\delta^{13}C$ differences caused by water stress (Weiguo et al. 2005; Diefendorf et al. 2010; Kohn 2010; Schulze et al. 2014) and other adaptive differences among species (e.g., Turner et al. 2008). Owing to the paucity of published data for arid Australia, the source dataset included a subset of 50 species mainly from southern African savannas. Published records of *n*-alkane $\delta^{13}C$ values (331 entries; 280 species) were restricted to taxa (mainly Genera, but also Family) found in the eastern Pilbara (*FloraBase*; www.florabase.dpaw.wa.gov.au).

Descriptive statistics of the arid zone C_3 and C_4 end-members used in the mixing model ($\delta^{13}C$ and abundance) were then compared with those of the full dataset incorporating non-Pilbara vegetation to validate subsequent interpretation. As would be expected, *n*-alkanes of the

terrestrial C_3 (n = 22) and C_4 (n = 32) plants formed distinct groupings within the $\delta^{13}C$ data set with minimum overlap (Table 1). Briefly, n-alkanes of C_3 plants had significantly ($p<0.005$) lower $\delta^{13}C$ values than C_4 in both the arid exclusive (C_3=−33.8 ± 2.0 ‰; C_4=−22.2 ± 2.2 ‰) and the full plant datasets (C_3=−34.7 ± 2.9 ‰; C_4=−24.2 ± 5.2 ‰). The average $\delta^{13}C$ values for the n-alkanes of C_3 and C_4 plants were both slightly higher and had smaller standard deviations in the arid dataset than the full dataset; however, this difference was not significant ($p>0.1$). Based on the same subset, we used an abundance matrix (Table 1) of the selected n-alkanes relative to one another (%) to account for the effect of concentration-dependence biases on mixing model estimates (Phillips and Koch 2002). The average n-alkane abundances calculated for C_3 or C_4 sources from the full datasets as well as the smaller subset of arid zone data were also consistently and significantly different (p-value<0.005), except for n-C_{27} (p=0.7) and n-C_{31} (p=0.06). In addition, n-$C_{27, 29}$ were more abundant in C_3 plants while n-$C_{31, 33}$ were more abundant in C_4 plants, and was most pronounced for arid species. However, there was no significant difference (p=0.06) in the relative abundance of the n-alkanes between the full and arid only datasets for either C_3 or C_4.

3. RESULTS

3.1 Organic matter composition

3.1.1 Bulk OC and solvent-extractable compounds

Sediment C and N abundances and stable isotope compositions are described in relation to each of the four hydroclimate periods described previously for this region: P1 (1–19 cm, CE 1990–2012), P2 (19–40 cm, CE 1600–1990), P3 (40–49 cm, CE 700–1600) and P4 (49–61 cm, CE <100–700). Total C was very low in all sediments (Table 2). TC content was highest in P1 (1.4 %) and lowest in P4 (< 0.4 %), with P2 (0.6 %) and P3 (0.7 %) between these values. Similarly, the highest N content as well as lowest $\delta^{15}N$ were found in P1 (0.12 % wt and 6.1 ‰). Conversely, the lowest N content

and highest δ^{15}N were found in P4 (0.01 % wt and 7.6 ‰). P2-P3 showed similar intermediate values (0.03 % wt and 7.4-7.5 ‰). The total solvent-extractable bitumen fraction (Table 2) of P1–P3 was 60 to 150 µg·g^{-1} of sediment, representing around 1 % of total C. Polar compounds dominated the bitumen (NSO - nitrogen, sulfur and oxygen polar compounds - fraction >89 %), whereas the aliphatic fractions were between 2 and 5 % (P3>P1>P2) and the aromatic fraction even smaller in P1 and P3 (<1 %). The aromatic fraction of P2 was relatively high at 8.5 %. The extractable fraction (i.e., bitumen) of P4 sediment was <5 µg· g^{-1} of sediment, which was insufficient for further characterisation. Sediment δ^{13}C values for the entire core were in the range -20.3 to -28.2 ‰, which are typical values of biologically sourced sedimentary OM (e.g., with mixed C_3/C_4 inputs) and imply negligible carbonate influence on measured δ^{13}C (Finlay and Kendall 2008).

3.1.2 Aliphatic hydrocarbon fractions

GC-MS analysis of the aromatic fractions yielded very few products; however, a wide distribution of aliphatic hydrocarbons were detected in the saturated fractions of P1–P3. The main aliphatic products included: *n*-alkanes, regular isoprenoids (e.g., phytane), branched alkanes and alkenes and saturated and unsaturated hopanoids and steroids. A particularly prominent homologous series of C_{17} to C_{35} *n*-alkanes accounted for ~60 to 85 % of the TIC signal of the saturate fraction, where *n*-C_{31} was the most dominant analyte (15–21 % of TIC; Fig. 2). The carbon preference index (CPI) was separately calculated for long-chain (C_{23} to C_{33}) *n*-alkanes (e.g., Bray and Evans 1961; Kuhn et al. 2010; Rao et al. 2008). The longer chain members showed a strong odd-over-even predominance ($CPI_{23–33}$ = 3–6; P2>P3>P1; Table 2). The P_{aq} values of P1–P3 were 0.1 or 0.3 suggesting the OM may mostly originate from macrophytes (Ficken et al. 2000). However, it is important to note that the P_{aq} value in sediment extracts likely reflect a mixture of inputs and may therefore also integrate a signal from both terrestrial and aquatic sources (Ficken et al. 2000). Less

abundant products across P1–P3 included a similar series of monounsaturated *n*-alkenes, as well as several branched alkanes including the regular isoprenoids pristine and phytane and polycyclic hopanoids and steroids. The hopanoids, best seen from the *m/z* 191 fragmentogram (Fig. 2 top), included C_{27} to C_{31} hopanes and even more abundant mono- and diunsaturated hopenes ($hC_{28–30=}$), tricyclic terpanes ($tC_{19–24}$) and the C_{24} tetracyclic terpane (TC_{24}). The steroids included C_{28} to C_{30} steranes ($sC_{28–30}$) as well as several short chain steranes ($sC_{19–22}$). The distribution of aliphatic products detected across sediment depths (P1–P3) were broadly similar. However, pristane and phytane were only detected in P1. The P1 sediments also showed a greater diversity, but lowest relative abundance, of hopanoid and steroid products. In contrast, *n*-alkenes were detected in P2 and P3 but not P1. Sediments of P2 had the highest representation of aliphatics other than *n*-alkanes. These were mainly linear branched alkanes and alkenes; short chain steranes ($sC_{19–22}$) were the major steroids of P1 (>50 % of *m/z* 217 steroid signal) while sterenes were particularly high in P2 and P3 (>80 % of *m/z* 217; Fig. 3).

3.1.3 $\delta^{13}C$ of n-*alkanes*

Stable carbon isotope values were measured for most *n*-alkanes detected in the P1–P3 samples (Table S1; Fig. 4). However, the concentrations of other aliphatic products were too low for accurate $\delta^{13}C$ measurement. The $\delta^{13}C$ value range for *n*-alkanes was mostly in a relatively narrow range around -29 ±2 ‰. Overall minimum $\delta^{13}C$ was −32.3 ± 0.1‰ (*n*-C_{17} in P1) and maximum $\delta^{13}C$ was −24.0 ‰ (*n*-C_{35} in P3). The $\delta^{13}C$ values of the mid-chain n-alkanes (*n*-$C_{21–26}$) were similar in P1 and P3, but higher by ~2 ‰ in P2. The odd n-alkanes had higher $\delta^{13}C$ values compared to their even carbon neighbours, particularly for the longer-chain compounds (>*n*-C_{27}) where this differential was as much as ~1‰ in sediments from for P2. The $\delta^{13}C$ values of the odd numbered *n*-alkanes from *n*-C_{27} followed the trend of P1<P2<P3 i.e., increasing with sediment depth and age (Fig. 4).

3.2 Sources of organic matter based on mixing model of long-chained *n*-alkanes

The mixing model based on $\delta^{13}C$ values of the long-chain odd *n*-alkanes (*n*-C_{27} to *n*-C_{33}) for P1–P3 is shown in Figure 5b. Typical of two-end member mixing models all probability distributions were unimodal (Parnell et al. 2010; Hopkians and Ferguson 2012; Fig. 5). The model suggests terrestrial C_3 dominance over recent decades (~20 years) (P1 median = 59 %; Table 2; Fig. 5), but with increasing importance of C_4 OM sources in the sediments of P2 (C_3 median = 53 %) to co-dominance of C_3 and C_4 sources in P3 (C_3 ~ C_4 = 50 %). The probability distributions for C_3 and C_4 are wide and overlapping indicating a high uncertainty with these estimates, however diverging median values suggests an increasing C_3 contribution and corresponding decrease in the C_4 with time (Fig. 5). While small aquatic and macrophytic inputs were detected in the molecular distributions, their contributions are unlikely to weight significantly on the mixing model estimates given the strong terrestrial plant signal of the abundant long-chain *n*-alkanes used here (see Discussion below).

4. DISCUSSION

4.1 The organic molecular and stable isotopic fingerprint of drylands

These results show that it is possible to extract organic molecular fossil distributions and $\delta^{13}C$ of *n*-alkanes from lake sediments of low OM content in tropical arid ecosystems. The low total C content of the Fortescue Marsh sediments (<1 %) reflects the inherently low OM contents of modern Pilbara soils and is typical of dry stream-bed sediments (Bennett and Adams 1999; Ford et al. 2007; McIntyre et al. 2009b). The low concentration of the extracted bitumens (60–150 μg· g^{-1} of bulk P1–P3 sediment; Table 2) is also typical of OM-poor environments and oligotrophic aquatic systems (e.g., Kristen et al. 2010; Pautler et al. 2010; Fang et al. 2014). Sub-aerial exposition of the sediment during prolonged dry periods over recent millennia (Rouillard et al. 2016) would also

have reduced OM preservation (Verschuren 1999). Nevertheless, saturated hydrocarbons typical of lipid metabolites were found in the upper 49 cm of the core (P1–P3; Fig. 2).

Our results also show that the molecular fossils can be used to characterise the major sources of sedimentary OM from the tropical arid system. The major aliphatic products identified in our sediments are indicative of predominantly terrestrial sources of OM at 14 Mile Pool (Fig. 2). The sediment of P1–3 consistently showed a homologous series of *n*-alkanes peaking at *n*-C_{31}. *n*-Alkanes are common hydrocarbon products of organic lake sediments derived from fatty acids, which are abundant components of epicuticular leaf waxes (Eglinton and Hamilton 1967) as well as many other biological systems and so are not always particularly source diagnostic of exact sources without additional evidence (e.g., stable isotopic composition). The relatively high abundances of *n*-alkanes in sediments across ecosystems are also due to a high structural recalcitrance to diagenesis (i.e., relatively high chemical stability, low solubility and are degraded slowly by microbes) compared to other functionalised biochemicals (Cranwell 1981; Schmidt et al. 2011). The unique lipid composition of many biological systems gives rise to *n*-alkanes of distinctive molecular distributions or stable isotope patterns that have thus been used previously to infer past hydroclimatic conditions across a range of environments (Castañeda and Schouten 2011; Garcin et al. 2012; Leng and Henderson 2013; Sun et al. 2013). For instance, chain length distribution can be used to distinguish algal (short chain) from terrestrial, higher plant (long chain) sources (Gelpi et al. 1970; Meyers and Ishiwatari 1993). A relatively high abundance of long chain *n*-alkanes (>*n*-C_{25}) is often attributed to a high flux (or persistence) of terrestrially-derived OM (Gelpi et al. 1970; Meyers and Ishiwatari 1993; Freeman and Colarusso 2001). While there are non-terrestrial sources of long chain *n*-alkanes e.g., *Botryococcus braunii*, a phytoplanktonic alga that is common in hypersaline or evaporitic lake settings (Grice et al. 1998), the long chain *n*-alkanes prominent in each of the P1–P3 sediments also showed a distinctive odd/even carbon

number preference ($CPI_{23–33}$ = 3–6; Fig. 2) typical of terrestrial plant sources (allochthonous; e.g., Meyers 1997; Volkman et al. 1998; Freeman and Colarusso 2001; Rao et al. 2008).

The *n*-alkanes detected in the P1–P3 sediments (*n*-C_{15-35} and CPI=2-12; Fig. 2 and Tables 2 & S1) had a similar distribution to those reported in many other arid zone lake deposits (e.g., Garcin et al. 2012). The $\delta^{13}C$ values were in the range −31 to −24 ‰ and displayed a 'saw-toothed' odd versus even carbon numbered pattern (Fig. 4) that is very typical of a leaf wax source and linked with higher plants biosynthesis (Collister et al. 1994; Zhou et al. 2010). The ephemeral reaches of low-lying rivers are often important sinks for the terrestrial OM of upper catchment rivers, streams and pools in arid environments (Jacobson et al. 2000; Fellman et al. 2013). Allochthonous material transported from the catchment through floods or wind is one of the main drivers of ecosystem metabolism in river networks (Sponseller et al. 2013). $\delta^{13}C$ of the 14 Mile Pool *n*-alkanes (−32.3 to −26.6 ‰ Fig. 4) are consistent with observations from modern sediments (−35.9 to −26.8 ‰) from the arid, Sudano-Sahelian shrub savannah zone of Cameroon (Garcin et al. 2012). The CPI values of long-chain *n*-alkanes from dryland soils can vary with aridity (Krull et al. 2006; Rao et al. 2008; Luo et al. 2012) and can extend to higher values than those reported here (e.g., 3–13, for *n*-C_{23}–*n*-C_{34} in several Chinese soils; Rao et al. 2008). Consequently, the molecular evidence from the 14 Mile Pool sediments records a clear and dominant signature of the terrestrial plant inputs from the surrounding arid catchment.

The shorter chain *n*-alkanes (*n*-$C_{17–26}$) of the sediments from 14 Mile Pool had lower $\delta^{13}C$ values than the more abundant long-chain *n*-alkanes (*n*-$C_{27–35}$), implying that these *n*-alkanes derive from a different source. The $\delta^{13}C$ of low MW *n*-alkanes (<*n*-C_{25}) in P1 and P3 were up to 1.5 ‰ lower than co-occurring odd numbered high MW *n*-alkanes (>*n*-C_{27}; Fig. 4). These lower $\delta^{13}C$ values are consistent with the lipids of algae or aquatic plants (Gelpi et al. 1970; Ficken et al. 2000), which

typically have lower $\delta^{13}C$ values than plant lipids (Chikaraishi and Naraoka 2003). Lower MW *n*-alkanes typically derive from lower trophic organisms and aquatic producers such as phytoplankton, benthic algae or aquatic macrophytes (e.g., Gelpi et al. 1970; Mead et al. 2005; Aichner et al. 2010; Garcin et al. 2012). Macrophyte input was also indicated by P_{aq} values of 0.1–0.3 for P1 and P3 sediments, though a mixture of the terrestrial and aquatic sources may also have contributed to this value (Ficken et al. 2000). In the P2 sediments, the P_{aq} value was in the same range (0.3) but the short chain *n*-alkanes were ~2 ‰ more positive than the long chain *n*-alkanes. The $\delta^{13}C$ values of the P2 sediments were also similar to the $\delta^{13}C$ values of *n*-alkanes reported for Lake Koucha sediments attributed to inputs from macrophytes and algae that had likely been influenced by higher $\delta^{13}C$ of bicarbonates in the water body (e.g., Aichner et al. 2010; Kristen et al. 2010). Speculatively, the heavier short-chain *n*-alkanes in P2 may suggest a relatively stronger groundwater influence during this period on the pool's hydrology and chemistry than present. This observation would be consistent with the occurrence of one or several extreme floods inferred for the periods (Rouillard et al. 2016), which would have enable an important rise in the water table (Skrzypek et al. 2013) and favourable conditions for macrophytic growth, i.e. prolonged inundation an a clear water column.

4.2 *n*-alkanes as proxies of ecosystem carbon stocks

By integrating the molecular abundance data with the Bayesian modelling of the stable isotopic composition of the *n*-alkanes, we can assess that our results reflect the major vegetation types in the catchment (C_3 and C_4) and hydrological processes at present and with hydroclimatic change through the late Holocene in this subtropical arid zone. The particularly high abundance of *n*-C_{31} in the sediments from 14 Mile Pool (Fig. 2) is consistent with the presently high catchment coverage and biomass of warm-climate adapted C_4 grasses (~64 % of mainly *Triodia* spp.) relative to that of woody C_3 plants, predominantly *Acacia* trees and shrubs (Fig. 1b; Adams et al. 2001). Though the

abundance of *n*-C_{31} alkane relative to *n*-C_{27} and *n*-C_{29} alkanes have been widely used to differentiate grass-type (C_4) versus woody (C_3) plant contributions, recent research has shown that caution is required with these estimates because the relative abundances of high molecular weight *n*-alkanes can vary for both functional types (Bush and McInerney 2013). At 14 Mile Pool, the occurrence of the very long-chain C_{33} (−26.6 ‰) and C_{35} (−24.0 ‰) *n*-alkanes and their relatively high $\delta^{13}C$ signatures (Cf. Ave ~−28.5 ‰ of *n*-$C_{33–35}$); Fig. 4) are further evidence of C_4 plant input to the P1-3 sediments. Very long-chain *n*-alkanes are not only generally more abundant in C_4 plants (e.g., Table 1), but their production may also be further enhanced under hot and dry conditions (Rommerskirchen et al. 2006; Vogts et al. 2009). The $\delta^{13}C$ of *n*-alkanes in Australian grassland soils usually reflects a C_4 prevalence (e.g., Krull et al. 2006).

The quantitative estimates from the stable isotope data suggests, however, the C_4 plants (41–50 % median contribution in mixing model) might not have contributed as considerably to the 14 Mile Pool sediments as might have been inferred from their current landscape dominance (64 % aboveground biomass; Table 2; Fig. 5). This is because the riparian vegetation of the 14 Mile Pool and broader riverine network (Fig. 1) may contribute substantial C_3 biomass resulting in a greater contribution of ^{13}C-depleted *n*-alkanes than might be expected from the non-riparian C_3 plant sources that predominantly inhabit arid environments. Disproportionally high riparian contributions to organic sediment loads have previously been reported in other grasslands dominated catchments: riparian trees in grasslands of sub-tropical Madagascar were thought responsible for sedimentary OM with $\delta^{13}C$ values more than 6 ‰ lower than predicted from the catchment vegetation composition (Marwick et al. 2014). Similarly, $\delta^{13}C$ trends in Holocene sediments from a stream channel in southeastern Arizona were attributed to the establishment of a riparian fringe and increasing contribution of C_3 herbaceous and woody vegetation over the modern dominance of C_4 perennial grasses (Biedenbender et al. 2004). Preferential deposition of

riparian tree leaves to lake sediment and the importance of lateral OM contribution to streams and rivers have also long been recognised in temperate environments (e.g., Conners and Naiman 1984; Seki et al. 2010). Viewed collectively, these findings suggest that the spatial structure of catchment vegetation, rather than the cover or biomass only, strongly affects terrestrial OM inputs to dryland sediments, and that the riparian contribution should particularly be taken into consideration when interpreting vegetation changes in arid environments from sediment *n*-alkanes $\delta^{13}C$.

If riparian plants (mainly C_3 and usually lower $\delta^{13}C$) are used as source material in the mixing model, however, this would also likely change the $\delta^{13}C$ values of the C_3 end member, resulting in a potential higher estimation of C_4 contribution to the Fortescue Marsh (Fig. 5). Response to plant water stress, observed both globally (Weiguo et al. 2005; Diefendorf et al. 2010; Kohn 2010) and along regional gradients (Schulze et al. 2014), can lead to an important $\delta^{13}C$ differential between riparian and to non-riparian C_3 sources (Fig. 5). A summary of $\delta^{13}C$ foliar signatures from woody C_3 plants of this study's region showed that species from riparian fringes in the Pilbara have significantly lower values (−4 ‰) than the foliage of homologue populations located on higher, more water-stressed, parts of the landscape (Table S2; Fig. 6). Thus, C_3-sourced *n*-alkanes with $\delta^{13}C$ values 4 ‰ lower than non-riparian sources would significantly decrease the model estimates for the C_3 contribution and correspondingly project a higher C_4 input. A further complication to consider is the substantial $\delta^{13}C$ offset that can occur between *n*-alkanes, leaf lipids and whole leaves (Rieley et al. 1993; Bi et al. 2005; Diefendorf et al. 2011; Codron et al. 2013). The $\delta^{13}C$ dynamics related to water availability such as local growth conditions (Schouten et al. 1998; Riebesell et al. 2000) and seasonal fluctuations (Lockheart et al. 1997) might also diverge for these entities, and there might also be variation of behaviour within phenology (Diefendorf et al. 2011), plant functional type (Shepherd and Wynne 2006; Bush and McInerney 2013; Cernusak et al.

2013), leaf ontogeny (Nguyen Tu et al. 2004) and phylogenetic group (Pedentchouk et al. 2008; Diefendorf et al. 2011).

In low water flow systems of arid zones, additional consideration of the complex deposition processes across timescales may be important from the reconstruction of past catchment vegetation from sediment records. For instance, leaf litter may accumulate in isolated pools or onto dry stream beds (McIntyre et al. 2009b) until transportation in various stages of decay downstream by heavy and unpredictable summer floods (e.g., Robertson et al. 2001; Francis and Sheldon 2002; Mladenov et al. 2007). Ecological 'booms' following large rains contrast prolonged periods of low productivity in arid catchments (Collins et al. 2008; McGrath et al. 2012; Kanniah et al. 2013). High energy floods in arid regions can lead to a wide dispersal of higher plants across the landscape and the increased likelihood following mortality of rapid photodegradation (i.e., minimal tree canopy or litter shelter from sustained UV radiation) or consumption by the termites prolific in Australian savannahs (e.g., Holt et al. 1987; Chen et al. 2003; Austin et al. 2004). The development of complementary indicators and of additional sediment records with finer temporal resolutions from the arid zone sediment may help towards a better understanding of these complex spatio-temporal patterns of OM deposition. Clearly, the range of $\delta^{13}C$ values for *n*-alkanes from different sources needs to be better defined in space and time for more precise quantitative mixing model estimates of contributions of different lipid sources to lake environments and reconstruction of vegetation cover in catchments.

The molecular data also showed a small but distinctive aquatic contribution in P1 that was not detected in older sediments (Fig. 2), particularly as determined from the lower chain length *n*-alkanes (Gelpi et al. 1970; Mead et al. 2005; Aichner et al. 2010; Garcin et al. 2012). The significantly lower $\delta^{13}C$ value of *n*-C_{17} compared to the larger *n*-alkanes (Fig. 4) further suggests a

cyanobacterial contribution to sediment OM (Kristen et al. 2010). Cyanobacterial mats are common in freshwater/brackish limnological conditions and high pH environments (Rontani and Volkman 2005) and microbial mats were visually evident at the sediment/water interface of the pool during several field surveys.

Steroids, generally originating from eukaryotic organisms such as higher plants or algae, as well as hopanoids, which are typically associated with microbial inputs (Aichner et al. 2010), were detected in all sediments. Their relative abundances were generally low (Fig. 3), though higher in P2 and P3 (steroids 7–8 % TIC signal; hopanoids 4–6 %) than P1 (steroids 1.3 %; hopanoids 2.6 %), perhaps on account of greater diagenetic reduction of the poly-hydroxy functionalities of their biochemical form (Peters et al. 2005). Sediments of P1 showed a more diverse assemblage of these products (Fig. 2 and 3), including unusual series of low molecular weight steranes ($C_{19–22}$) and tri- and tetracyclic terpanes (C_{19}–C_{24}). The greater biomarker diversity evident in P1 suggests the recent wetter conditions (Rouillard et al. 2016) favoured a more complex microbial pool that may also have supported greater heterotroph reworking of the OM (i.e., resulting in overall lower abundance). A similar series of low molecular weight steranes (extending to slightly large Cn) were reported in relatively high concentrations in immature evaporitic marl sediments of the Jinxian Sag, Bohai Bay Basin, North China (Lu et al. 2009) and generally attributed to early diagenetic products of microbial sources in a carbonate environment (Erik 2011; Oliveira et al. 2012). The higher steroid to hopanoid ratio detected in P2 and P3 (Fig. 3) is also consistent with a greater representation of terrestrially-derived OM during those periods compared to the more recent P1 sediments (Tissot and Welte 1984).

4.3 Do sediment *n*-alkanes reflect hydroclimatic change at the Fortescue Marsh in the late Holocene?

The final objective of this study was to assess whether the distribution of biomarkers and $\delta^{13}C$ values of *n*-alkanes from the sediment reflected ecosystem responses to regional hydroclimatic change over the late Holocene (last ~2000 years). We have previously discussed our molecular record against the hydroclimatic reconstruction at the Fortescue Marsh (Rouillard et al., 2016), and here compare our findings to other regional palaeoecological records focussing on OM and vegetation changes for the four periods investigated (P1-P4). The very low organic content of the older section (P4) core—below the detection limit of presently applied GC-MS analyses—is consistent with notably drier conditions in the inland Pilbara region more than 1300 years ago compared to present (Rouillard et al. 2016). Marine sediment pollen records (van der Kaars et al. 2006) and coastal speleothem records (Denniston et al. 2013) have revealed a decrease in C_3 vegetation across northwest Australia since the mid-Holocene, which has been attributed to a drier climate, equivalent to a decrease of ~150 mm·year^{-1} in mean coastal rainfall. Terrestrial pollen records further east also suggest a decline in effective precipitation (EP) in tropical northern Australia (Gulf of Carpenteria) from 4000–3500 years BP followed by an increase in EP over the last 2000 years (Shulmeister and Lees 1995). Recent evaluation of a sediment record from the eastern Kimberley has also indicated increasing woody vegetation following rapid increased fluvial sedimentation around CE 650–850 (McGowan et al. 2012).

Given the differences evident in the molecular and stable isotopic distributions of lipid derived *n*-alkanes in sediments from the oldest (P3) to the youngest (P1), we might conclude that vegetation structure and composition in the catchment have been broadly consistent in the region for the last ~1300 years (Table 2; Fig. 2). Nonetheless, other hydroclimatic reconstructions based on physical and other biogeochemical characteristics indicate conditions in the region have become

progressively wetter since ~ CE 700 (Rouillard et al. 2016). In particular, the near-permanently inundated conditions at the site under a wetter recent climate in the last ~20 years is evident from multiple sediment indicators from this sequence (P1; Rouillard et al. 2016) that are corroborated by instrumental data and modelling from satellite imagery and rainfall timeseries (Rouillard et al. 2015; Shi et al. 2008). Under wetter (or less arid) conditions we might expect i) an expanded riparian fringe; ii) greater productivity of C_3 trees and shrubs; and/or iii) alleviated water stress of this vegetation. Such a scenario would account for the significantly lower $\delta^{13}C$ values evident in the shallower sediment (P1 < P2 < P3; total variance of ~2 ‰; Fig. 5). Similar 2–3 ‰ magnitude shifts in the $\delta^{13}C$ values of long ($C_{29–33}$) odd chain *n*-alkanes extracted from Lake Malawi sediments, equatorial East Africa, was reported to reflect a 15 % increase in C_4 vegetation and millennial drought during the Younger Dryas cold period (Castañeda et al. 2007). A 2–3 ‰ shift in the $\delta^{13}C$ of long chain *n*-alkanoic acids extracted from marine sediment was also associated to a ~20 % variability in the C_3 and C_4 vegetation of northeast Africa (Feakins et al. 2007). We thus conclude that sediment biomarkers and *n*-alkanes $\delta^{13}C$ values from the 14 Mile Pool effectively reflected the local response of vegetation to hydrological and regional hydroclimatic change in the late Holocene, even though this change may have been relatively modest on a catchment scale. Taken together, our results show that improved baseline data and a careful consideration of the complex spatial and temporal interaction between plants and water in arid tropical ecosystems are crucial for an appropriate interpretation of past vegetation dynamics from molecular proxies.

5. CONCLUSIONS

The major sedimentary organic inputs of an episodic wetland (Fortescue Marsh, Pilbara), including aquatic microflora, C_4 grasses, and C_3 plants originating at least partly from a significant riparian fringe, could be revealed from the distributions and $\delta^{13}C$ values of aliphatic hydrocarbon compounds (including *n*-alkanes, branched alkanes, hopanoids and steroids) detected from them in trace levels. A temporal flux of some sources was also evident. The stable isotopic signatures measured for several of the more abundant *n*-alkanes provided additional C source information that can be useful for paleoclimate reconstructions. Particularly, the relatively lower $\delta^{13}C$ values of long chain *n*-alkanes in modern sediments reflected the emergence of wetter conditions through the late Holocene, and particularly over recent decades. Though we highlight limitations and caution in interpreting organic geochemical signals in sediments from tropical drylands, this approach provides valuable information for the interpretation of arid paleoenvironmental records globally. Of note, these data can serve as relatively modern analogues for the characteristics of biomarker records that have been deposited during ancient dry phases recorded in very long (>100,000 yrs) paleoenvironmental records, such as the ongoing projects of the International Continental Scientific Drilling Program (http://www.icdp-online.org/home/): the Hominin Sites and Paleolakes Drilling Project (HSPDP) in East Africa, the Lake Chad Deep Drilling (CHADRILL) in North Africa, the Lake Petén Itza in Guatemala and the Lake Chalco in Mexico. Regionally, more extensive and representative organic geochemical datasets, particularly of *n*-alkane $\delta^{13}C$ signatures from a range of sources (e.g. riparian vegetation) common across northern and inland Australia and other sub-tropical drylands, will help improve the accuracy and uncertainty of mixing models to reconstruct past vegetation contributions quantitatively in these relatively underrepresented regions.

ACKNOWLEDGEMENTS

We thank D. Thomas (Oxford Uni.), D. Vershuren (Ghent Uni.) and J. Tibby (Uni. Adelaide) for their comments, which contributed to improve the manuscript. This research was supported by the Australian Research Council (ARC) in partnership with Rio Tinto (LP120100310). A. Rouillard was supported by the Australian Government and UWA via an International Postgraduate Research Scholarships (IPRS), Australian Postgraduate Award (APA) and a UWA Safety Top-up Scholarship, as well as by the Canadian and Québec governments via a Natural Sciences and Engineering Research Council (NSERC) and Fonds québécois de la recherche sur la nature et les technologies (FQRNT) graduate scholarships. G. Skrzypek participation was supported by an ARC Future Fellowship (FT110100352). K. Grice participation was supported by an ARC DORA fellowship (DP130100577) and ARC LIEFP grant for CSIA. Data for Fig. 6 (Table S2) were cumulatively collected by Ecosystem Research Group members R. Argus, L. Cullen, J. Graham, P. Landman, R. McIntyre, E. McLean and G. Page. Laboratory support at Curtin University was kindly provided by Robert Lockhart and the WA-OIGC team. Glenn Kirkpatrick and Douglas Ford provided invaluable support in the field (UWA). We also thank Adrienne Marquis (DPaw) for her contribution of plant survey information from the Fortescue Marsh. We ultimately acknowledge the kind field support of Murray and Ray Kennedy (Roy Hill Station), Sue and Lee Bickell (Marillana Station), Barry and Bella Grett (Ethel Creek Station) and Victor and Larissa Gleeson (Mulga Downs Station).

REFERENCES

Adams M, Grierson P, Bussau A, Dorling K (2001) Biomass and carbon in vegetation of the Pilbara region, Western Australia. Dissertation, The University of Western Australia

Aichner B, Wilkes H, Herzschuh U, Mischke S, Zhang C (2010) Biomarker and compound-specific $\delta^{13}C$ evidence for changing environmental conditions and carbon limitation at Lake Koucha, eastern Tibetan Plateau. Journal of Paleolimnology 43:873–899

Argus RE, Colmer TD, Grierson PF (2015) Early physiological flood tolerance is followed by slow post-flooding root recovery in the dryland riparian tree *Eucalyptus camaldulensis* subsp. *refulgens*. Plant, Cell & Environment 38:1189–1199

Argus R, Page G, Grierson P (2014) Impacts of artificial inundation of ephemeral creek beds on mature riparian eucalypts in semi-arid northwest Australia. EGU General Assembly Conference Abstracts 16:10098

Atahan P, Heijnis H, Dodson J, Grice K, Le M, Pierre, Taffs K, Hembrow S, Woltering M, Zawadzki A (2015) Pollen, biomarker and stable isotope evidence of late Quaternary environmental change at Lake McKenzie, southeast Queensland. Journal of Paleolimnology 53:139–156

Austin AT, Yahdjian L, Stark JM, Belnap J, Porporato A, Norton U, Ravetta DA, Schaeffer SM (2004) Water pulses and biogeochemical cycles in arid and semiarid ecosystems. Oecologia 141:221–235

Barr C, Tibby J, Gell P, Tyler J, Zawadzki A, Jacobsen GE (2014) Climate variability in south-eastern Australia over the last 1500 years inferred from the high-resolution diatom records of two crater lakes. Quaternary Science Reviews 95:115–131

Battin TJ, Kaplan LA, Findlay S, Hopkinson CS, Marti E, Packman AI, Newbold JD, Sabater F (2008) Biophysical controls on organic carbon fluxes in fluvial networks. Nature Geoscience 1:95–100

Beard JS (1975) The vegetation of the Pilbara area. Vegetation Survey of Western Australia 1:1 000 000 Vegetation Series, Map and explanatory notes

Bennett LT, Adams MA (2001) Response of a perennial grassland to nitrogen and phosphorus additions in sub-tropical, semi-arid Australia. Journal of Arid Environments 48:289–308

Bessems I, Verschuren D, Russell JM, Hus J, Mees F, Cumming BF (2008) Palaeolimnological evidence for widespread late 18th century drought across equatorial East Africa. Palaeogeography, Palaeoclimatology, Palaeoecology 259:107–120

Bi X, Sheng G, Liu X, Li C, Fu J (2005) Molecular and carbon and hydrogen isotopic composition of *n*-alkanes in plant leaf waxes. Organic Geochemistry 36:1405–1417

Biedenbender SH, McClaran MP, Quade J, Weltz MA (2004) Landscape patterns of vegetation change indicated by soil carbon isotope composition. Geoderma 119:69–83

Birks HJB, Birks HH (2016) How have studies of ancient DNA from sediments contributed to the reconstruction of Quaternary floras? New Phytologist 209:499–506

Blumer M (1957) Removal of elemental sulfur from hydrocarbon fractions. Analytical Chemistry 29:1039–1041

Bray EE, Evans ED (1961) Distribution of *n*-paraffins as a clue to recognition of source beds. Geochimica et Cosmochimica Acta 22:2–15

Brodie CR, Casford JSL, Lloyd JM, Leng MJ, Heaton THE, Kendrick CP, Yongqiang Z (2011) Evidence for bias in C/N, δ^{13}C and δ^{15}N values of bulk organic matter, and on environmental

interpretation, from a lake sedimentary sequence by pre-analysis acid treatment methods. Quaternary Science Reviews 30:3076–3087

Bush RT, McInerney FA (2013) Leaf wax *n*-alkane distributions in and across modern plants: Implications for paleoecology and chemotaxonomy. Geochimica et Cosmochimica Acta 117:161–179

Carolin RC, Jacobs SWL, Vesk M (1982) The chlorenchyma of some members of the Salicornieae (Chenopodiaceae). Australian Journal of Botany 30:387–392

Castañeda IS, Werne JP, Johnson TC, Filley TR (2009a) Late Quaternary vegetation history of southeast Africa: The molecular isotopic record from Lake Malawi. Palaeogeography, Palaeoclimatology, Palaeoecology 275:100–112

Castañeda IS, Mulitza S, Schefuß E, dos Santos RAL, Damsté JSS, Schouten S (2009b) Wet phases in the Sahara/Sahel region and human migration patterns in North Africa. Proceedings of the National Academy of Sciences 106:20159–20163

Castañeda IS, Schouten S (2011) A review of molecular organic proxies for examining modern and ancient lacustrine environments. Quaternary Science Reviews 30:2851–2891

Castañeda IS, Werne JP, Johnson TC (2007) Wet and arid phases in the southeast African tropics since the Last Glacial Maximum. Geology 35:823–826

Cernusak LA, Ubierna N, Winter K, Holtum JAM, Marshall JD, Farquhar GD (2013) Environmental and physiological determinants of carbon isotope discrimination in terrestrial plants. New Phytologist 200:950–965

Chen X, Hutley LB, Eamus D (2003) Carbon balance of a tropical savanna of northern Australia. Oecologia 137:405–416

Chikaraishi Y, Naraoka H (2003) Compound-specific δD-δ^{13}C analyses of *n*-alkanes extracted from terrestrial and aquatic plants. Phytochemistry 63:361–371

Codron J, Lee-Thorp JA, Sponheimer M, Codron D (2013) Plant stable isotope composition across habitat gradients in a semi-arid savanna: implications for environmental reconstruction. Journal of Quaternary Science 28:301–310

Collins SL, Sinsabaugh RL, Crenshaw C, Green L, Porras-Alfaro A, Stursova M, Zeglin LH (2008) Pulse dynamics and microbial processes in aridland ecosystems. Journal of Ecology 96:413–420

Collister JW, Rieley G, Stern B, Eglinton G, Fry B (1994) Compound-specific δ^{13}C analyses of leaf lipids from plants with differing carbon dioxide metabolisms. Organic Geochemistry 21:619–627

Conners ME, Naiman RJ (1984) Particulate allochthonous inputs: relationships with stream size in an undisturbed watershed. Canadian Journal of Fisheries and Aquatic Sciences 41:1473–1484

Cranwell PA (1981) Diagenesis of free and bound lipids in terrestrial detritus deposited in a lacustrine sediment. Organic Geochemistry 3:79–89

Cullen LE, Adams MA, Anderson MJ, Grierson PF (2008) Analyses of δ^{13}C and δ^{18}O in tree rings of *Callitris columellaris* provide evidence of a change in stomatal control of photosynthesis in response to regional changes in climate. Tree Physiology 28:1525–1533

Cushing EJ (1967) Evidence for differential pollen preservation in late Quaternary sediments in Minnesota. Review of Palaeobotany and Palynology 4:87–101

Denniston RF, Asmerom Y, Lachniet M, Polyak VJ, Hope P, An N, Rodzinyak K, Humphreys WF (2013) A Last Glacial Maximum through middle Holocene stalagmite record of coastal Western Australia climate. Quaternary Science Reviews 77:101–112

Diefendorf AF, Freeman KH, Wing SL, Graham HV (2011) Production of *n*-alkyl lipids in living plants and implications for the geologic past. Geochimica et Cosmochimica Acta 75:7472–7485

Diefendorf AF, Mueller KE, Wing SL, Koch PL, Freeman KH (2010) Global patterns in leaf ^{13}C discrimination and implications for studies of past and future climate. Proceedings of the National Academy of Sciences 107:5738–5743

Duan Y, Wu Y, Cao X, Zhao Y, Ma L (2014) Hydrogen isotope ratios of individual *n*-alkanes in plants from Gannan Gahai Lake (China) and surrounding area. Organic Geochemistry 77:96–105

Dubois N, Oppo DW, Galy VV, Mohtadi M, van dK, Sander, Tierney JE, Rosenthal Y, Eglinton TI, Lückge A, Linsley BK (2014) Indonesian vegetation response to changes in rainfall seasonality over the past 25,000 years. Nature Geoscience 4:513–517

Eglinton G, Hamilton RJ (1967) Leaf epicuticular waxes. Science 156:1322–1335

Erik YN (2011) Hydrocarbon generation potential and Miocene—Pliocene paleoenvironments of the Kangal Basin (Central Anatolia, Turkey). Journal of Asian Earth Sciences 42:1146–1162

Fang J, Wu F, Xiong Y, Li F, Du X, An D, Wang L (2014) Source characterization of sedimentary organic matter using molecular and stable carbon isotopic composition of *n*-alkanes and fatty acids in sediment core from Lake Dianchi, China. Science of The Total Environment 473:410–421

Feakins SJ, Eglinton TI, demenocal PB (2007) A comparison of biomarker records of northeast African vegetation from lacustrine and marine sediments (ca. 3.40 Ma). Organic Geochemistry 38:1607–1624

Fellman JB, Petrone KC, Grierson PF (2013) Leaf litter age, chemical quality, and photodegradation control the fate of leachate dissolved organic matter in a dryland river. Journal of Arid Environments 89:30–37

Ficken KJ, Li B, Swain DL, Eglinton G (2000) An *n*-alkane proxy for the sedimentary input of submerged/floating freshwater aquatic macrophytes. Organic Geochemistry 31:745–749

Finlay JC, Kendall C (2008) Stable isotope tracing of temporal and spatial variability in organic matter sources to freshwater ecosystems. In: Michener R, Lajtha K (eds) Stable isotopes in ecology and environmental science. Wiley-Blackwell, Hoboken, Oxford, UK, pp 283-333

Ford DJ, Cookson WR, Adams MA, Grierson PF (2007) Role of soil drying in nitrogen mineralization and microbial community function in semi-arid grasslands of north-west Australia. Soil Biology and Biochemistry 39:1557–1569

Francis C, Sheldon F (2002) River Red Gum (*Eucalyptus camaldulensis* Dehnh.) organic matter as a carbon source in the lower Darling River, Australia. Hydrobiologia 481:113–124

Freeman KH, Colarusso LA (2001) Molecular and isotopic records of C4 grassland expansion in the late Miocene. Geochimica et Cosmochimica Acta 65:1439–1454

Garcin Y, Schwab VF, Gleixner G, Kahmen A, Todou G, Séné O, Onana JM, Achoundong G, Sachse D (2012) Hydrogen isotope ratios of lacustrine sedimentary *n*-alkanes as proxies of tropical African hydrology: Insights from a calibration transect across Cameroon. Geochimica et Cosmochimica Acta 79:106–126

Gelpi E, Schneider H, Mann J, Oro J (1970) Hydrocarbons of geochemical significance in microscopic algae. Phytochemistry 9:603–612

Gergis J, Hope P, Abram N, Henley B (2014) Australasia's climate variability: clues drawn from paleoclimate and model data over the last 2000 years. PAGES Magazine 22:101

Grice K, Schouten S, Nissenbaum A, Charrach J, Sinninghe D, Jaap S (1998) A remarkable paradox: sulfurised freshwater algal (*Botryococcus braunii*) lipids in an ancient hypersaline euxinic ecosystem. Organic Geochemistry 28:195–216

Hoffmann B, Kahmen A, Cernusak LA, Arndt SK, Sachse D (2013) Abundance and distribution of leaf wax *n*-alkanes in leaves of *Acacia* and *Eucalyptus* trees along a strong humidity gradient in northern Australia. Organic Geochemistry 62:62–67

Holt JA (1987) Carbon mineralization in semi-arid northeastern Australia: the role of termites. Journal of Tropical Ecology 3:255–263

Hopkins JB, Ferguson JM (2012) Estimating the diets of animals using stable isotopes and a comprehensive Bayesian mixing model. PLoS One 7:e28478

Huxman TE, Snyder KA, Tissue D, Leffler AJ, Ogle K, Pockman WT, Sandquist DR, Potts DL, Schwinning S (2004) Precipitation pulses and carbon fluxes in semiarid and arid ecosystems. Oecologia 141:254–268

Jacobson PJ, Jacobson KM, Angermeier PL, Cherry DS (2000) Variation in material transport and water chemistry along a large ephemeral river in the Namib Desert. Freshwater Biology 44:481–491

Kanniah KD, Beringer J, Hutley LB (2013) Response of savanna gross primary productivity to interannual variability in rainfall: Results of a remote sensing based light use efficiency model. Progress in Physical Geography 37:642–663

Kennard MJ, Pusey BJ, Olden JD, Mackay SJ, Stein JL, Marsh N (2010) Classification of natural flow regimes in Australia to support environmental flow management. Freshwater Biology 55:171–193

Kohn MJ (2010) Carbon isotope compositions of terrestrial C3 plants as indicators of (paleo) ecology and (paleo) climate. Proceedings of the National Academy of Sciences 107:19691–19695

Kristen I, Wilkes H, Vieth A, Zink K-G, Plessen B, Thorpe J, Partridge TC, Oberhänsli H (2010) Biomarker and stable carbon isotope analyses of sedimentary organic matter from Lake Tswaing: evidence for deglacial wetness and early Holocene drought from South Africa. Journal of Paleolimnology 44:143–160

Krull E, Sachse D, Mügler I, Thiele A, Gleixner G (2006) Compound-specific $\delta^{13}C$ and $\delta^{2}H$ analyses of plant and soil organic matter: A preliminary assessment of the effects of vegetation change on ecosystem hydrology. Soil Biology and Biochemistry 38:3211–3221

Krull ES, Skjemstad JO, Burrows WH, Bray SG, Wynn JG, Bol R, and S, Leonie, Harms B (2005) Recent vegetation changes in central Queensland, Australia: Evidence from $\delta^{13}C$ and ^{14}C analyses of soil organic matter. Geoderma 126:241–259

Kuhn TK, Krull ES, Bowater A, Grice K, Gleixner G (2010) The occurrence of short chain *n*-alkanes with an even over odd predominance in higher plants and soils. Organic Geochemistry 41:88–95

Leng MJ, Henderson ACG (2013) Recent advances in isotopes as palaeolimnological proxies. Journal of Paleolimnology 49:481–496

Lockheart MJ, Van B, Pim F, Evershed RP (1997) Variations in the stable carbon isotope compositions of individual lipids from the leaves of modern angiosperms: implications for the study of higher land plant-derived sedimentary organic matter. Organic Geochemistry 26:137–153

Lowe JJ (1982) Three Flandrian Pollen Profiles from the Teith Valley, Perthshire, Scotland. II. Analysis of Deteriorated Pollen. New Phytologist 90:371–385

Lu H, Chen T, Grice K, Greenwood P, Peng P, Sheng G (2009) Distribution and significance of novel low molecular weight sterenes in an immature evaporitic sediment from the Jinxian Sag, North China. Organic Geochemistry 40:902–911

Luo P, Peng P, Lü H, Zheng Z, Wang X (2012) Latitudinal variations of CPI values of long-chain *n*-alkanes in surface soils: Evidence for CPI as a proxy of aridity. Science China Earth Sciences 55:1134–1146

Marwick TR, Borges AV, Van A, Kristof, Darchambeau F, Bouillon S (2014) Disproportionate Contribution of Riparian Inputs to Organic Carbon Pools in Freshwater Systems. Ecosystems 17:974–989

McGowan H, Marx S, Moss P, Hammond A (2012) Evidence of ENSO mega-drought triggered collapse of prehistory Aboriginal society in northwest Australia. Geophysical Research Letters 39:L22702, 1–5

McGrath GS, Sadler R, Fleming K, Tregoning P, Hinz C, Veneklaas EJ (2012) Tropical cyclones and the ecohydrology of Australia's recent continental-scale drought. Geophysical Research Letters 39:L03404, 1–16

McIntyre RES, Adams MA, Ford DJ, Grierson PF (2009a) Rewetting and litter addition influence mineralisation and microbial communities in soils from a semi-arid intermittent stream. Soil Biology and Biochemistry 41:92–101

McIntyre RES, Adams MA, Grierson PF (2009b) Nitrogen mineralization potential in rewetted soils from a semi-arid stream landscape, north-west Australia. Journal of Arid Environments 73:48–54

McKenzie NL, van Leeuwen S, Pinder AM (2009) Introduction to the Pilbara biodiversity survey, 2002-2007. Records of the Western Australian Museum, Supplement 78:3–89

McKirdy DM, Thorpe CS, Haynes DE, Grice K, Krull ES, Halverson GP, Webster LJ (2010) The biogeochemical evolution of the Coorong during the mid-to late Holocene: An elemental, isotopic and biomarker perspective. Organic Geochemistry 41:96–110

Mead R, Xu Y, Chong J, Jaffé R (2005) Sediment and soil organic matter source assessment as revealed by the molecular distribution and carbon isotopic composition of *n*-alkanes. Organic Geochemistry 36:363–370

Meyers PA (1997) Organic geochemical proxies of paleoceanographic, paleolimnologic, and paleoclimatic processes. Organic Geochemistry 27:213–250

Meyers PA, Ishiwatari R (1993) Lacustrine organic geochemistry-an overview of indicators of organic matter sources and diagenesis in lake sediments. Organic Geochemistry 20:867–900

Mladenov N, McKnight DM, Wolski P, Murray-Hudson M (2007) Simulation of DOM fluxes in a seasonal floodplain of the Okavango Delta, Botswana. Ecological Modelling 205:181–195

Moir-Barnetson L (2014) Ecophysiological responses to changes in salinity and water availability in stem-succulent halophytes (*Tecticornia* spp.) from an ephemeral salt lake. Plant Biology, Ph.D., The University of Western Australia, 208 pp.

Nguyen Tu TT, Derenne S, Largeau C, Bardoux G, Mariotti A (2004) Diagenesis effects on specific carbon isotope composition of plant *n*-alkanes. Organic Geochemistry 35:317–329

O'Donnell AJ, Boer MM, McCaw WL, Grierson PF (2011) Climatic anomalies drive wildfire occurrence and extent in semi-arid shrublands and woodlands of southwest Australia. Ecosphere 2:Art127, 1–15

Oliveira CR, Ferreira AA, Oliveira CJF, Azevedo DA, Santos N, Eugênio V, Aquino N, Francisco R (2012) Biomarkers in crude oil revealed by comprehensive two-dimensional gas

chromatography time-of-flight mass spectrometry: depositional paleoenvironment proxies. Organic Geochemistry 46:154–164

Pagès A, Grice K, Ertefai T, Skrzypek G, Jahnert R, Greenwood P (2014) Organic geochemical studies of modern microbial mats from Shark Bay: Part I: Influence of depth and salinity on lipid biomarkers and their isotopic signatures. Geobiology 12:469–487

Pagès A, Grice K, Welsh DT, Teasdale PT, Van K, Martin J, Greenwood P (2015) Lipid Biomarker and Isotopic Study of Community Distribution and Biomarker Preservation in a Laminated Microbial Mat from Shark Bay, Western Australia. Microbial Ecology 70:459–472

Parnell AC, Inger R, Bearhop S, Jackson AL (2010) Source partitioning using stable isotopes: coping with too much variation. PLOS one 5:e9672

Pautler BG, Austin J, Otto A, Stewart K, Lamoureux SF, Simpson MJ (2010) Biomarker assessment of organic matter sources and degradation in Canadian High Arctic littoral sediments. Biogeochemistry 100:75–87

Pedentchouk N, Sumner W, Tipple B, Pagani M (2008) δ^{13}C and δD compositions of *n*-alkanes from modern angiosperms and conifers: An experimental set up in central Washington State, USA. Organic Geochemistry 39:1066–1071

Peters KE, Walters CC, Moldowan JM (2005) (eds) The biomarker guide: Volume 1, Biomarkers and isotopes in the environment and human history. Cambridge University Press, Cambridge, 471 pp

Phillips DL, Koch PL (2002) Incorporating concentration dependence in stable isotope mixing models. Oecologia 130:114–125

Puttock A, Dungait JAJ, Bol R, and D, Elizabeth R, Macleod CJA, Brazier RE (2012) Stable carbon isotope analysis of fluvial sediment fluxes over two contrasting C4-C3 semi-arid vegetation transitions. Rapid Communications in Mass Spectrometry 26:2386–2392

Qin C, Yang B, Bräuning A, Grießinger J, Wernicke J (2015) Drought signals in tree-ring stable oxygen isotope series of Qilian juniper from the arid northeastern Tibetan Plateau. Global and Planetary Change 125:48–59

Rao Z, Jia G, Zhu Z, Wu Y, Zhang J (2008) Comparison of the carbon isotope composition of total organic carbon and long-chain *n*-alkanes from surface soils in eastern China and their significance. Chinese Science Bulletin 53:3921–3927

Reid MA, Ogden R, Thoms MC (2011) The influence of flood frequency, geomorphic setting and grazing on plant communities and plant biomass on a large dryland floodplain. Journal of Arid Environments 75:815–826

Riebesell U, Revill AT, Holdsworth DG, Volkman JK (2000) The effects of varying CO2 concentration on lipid composition and carbon isotope fractionation in *Emiliania huxleyi*. Geochimica et Cosmochimica Acta 64:4179–4192

Rieley G, Collister JW, Stern B, Eglinton G (1993) Gas chromatography/isotope ratio mass spectrometry of leaf wax *n*-alkalines from plants of differing carbon dioxide metabolisms. Rapid Communications in Mass Spectrometry 7:488–491

Robertson AI, Bacon P, Heagney G (2001) The responses of floodplain primary production to flood frequency and timing. Journal of Applied Ecology 38:126–136

Romero-Viana L, Kienel U, Sachse D (2012) Lipid biomarker signatures in a hypersaline lake on Isabel Island (Eastern Pacific) as a proxy for past rainfall anomaly (1942-2006AD). Palaeogeography, Palaeoclimatology, Palaeoecology 350-352:49–61

Rommerskirchen F, Plader A, Eglinton G, Chikaraishi Y, Rullkötter J (2006) Chemotaxonomic significance of distribution and stable carbon isotopic composition of long-chain alkanes and alkan-1-ols in C4 grass waxes. Organic Geochemistry 37:1303–1332

Rontani J-F, Volkman JK (2005) Lipid characterization of coastal hypersaline cyanobacterial mats from the Camargue (France). Organic Geochemistry 36:251–272

Rouillard A, Skrzypek G, Dogramaci S, Turney C, Grierson PF (2015) Impacts of high inter-annual variability of rainfall on a century of extreme hydrologic regime of northwest Australia. Hydrology and Earth System Sciences 19:2057–2078

Rouillard, A, Skrzypek, G, Turney, C, Dogramaci, S, Hua, Q, Zawadzki, A, Reeves, J, O'Donnell, A, and Grierson, P (2016). Evidence for 'megafloods' in arid subtropical Western Australia during the Little Ice Age Chronozone. Quaternary Science Reviews 144:107 – 122

Sachse D, Billault I, Bowen GJ, Chikaraishi Y, Dawson TE, Feakins SJ, Freeman KH, Magill CR, McInerney FA, van dM, Marcel T.J., Polissar P, Robins RJ, Sachs JP, Schmidt H-L, Sessions AL, White JWC, West JB, Kahmen A (2012) Molecular Paleohydrology: Interpreting the Hydrogen-Isotopic Composition of Lipid Biomarkers from Photosynthesizing Organisms. Annual Review of Earth and Planetary Sciences 40:221–249

Sachse D, Sachs JP (2008) Inverse relationship between D/H fractionation in cyanobacterial lipids and salinity in Christmas Island saline ponds. Geochimica et Cosmochimica Acta 72:793–806

Sage RF, Christin P-A, Edwards EJ (2011) The C4 plant lineages of planet Earth. Journal of Experimental Botany 62:3155–3169

Schmidt MWI, Torn MS, Abiven S, Dittmar T, Guggenberger G, Janssens IA, Kleber M, Kögel-Knabner I, Lehmann J, Manning DAC, others (2011) Persistence of soil organic matter as an ecosystem property. Nature 478:49–56

Schouten S, Klein B, Wim, Blokker P, Schogt N, Rijpstra WIC, Grice K, Baas M, Sinninghe D, Jaap S (1998) Biosynthetic effects on the stable carbon isotopic compositions of algal lipids: Implications for deciphering the carbon isotopic biomarker record. Geochimica et Cosmochimica Acta 62:1397–1406

Schulze ED, Nicolle D, Boerner A, Lauerer M, Aas G, Schulze I (2014) Stable carbon and nitrogen isotope ratios of *Eucalyptus* and *Acacia* species along a seasonal rainfall gradient in Western Australia. Trees 28:1125–1135

Schwinning S, Sala OE, Loik ME, Ehleringer JR (2004) Thresholds, memory, and seasonality: understanding pulse dynamics in arid/semi-arid ecosystems. Oecologia 141:191–193

Seki O, Nakatsuka T, Shibata H, Kawamura K (2010) A compound-specific *n*-alkane δ^{13}C and δD approach for assessing source and delivery processes of terrestrial organic matter within a forested watershed in northern Japan. Geochimica et Cosmochimica Acta 74:599–613

Shepherd T, Wynne G, D (2006) The effects of stress on plant cuticular waxes. New Phytologist 171:469–499

Shi G, Cai W, Cowan T, Ribbe J, Rotstayn L, Dix M (2008) Variability and trend of North West Australia rainfall: observations and coupled climate modeling. Journal of Climate 21:2938–2959

Shulmeister J, Lees BG (1995) Pollen evidence from tropical Australia for the onset of an ENSO-dominated climate at c. 4000 BP. The Holocene 5:10–18

Skrzypek G (2013) Normalization procedures and reference material selection in stable HCNOS isotope analyses: an overview. Analytical and bioanalytical chemistry 405:2815–2823

Skrzypek G, Dogramaci S, Grierson PF (2013) Geochemical and hydrological processes controlling groundwater salinity of a large inland wetland of northwest Australia. Chemical Geology 357:164–177

Snyder KA, Tartowski SL (2006) Multi-scale temporal variation in water availability: implications for vegetation dynamics in arid and semi-arid ecosystems. Journal of Arid Environments 65:219–234

Sponseller RA, Heffernan JB, Fisher SG (2013) On the multiple ecological roles of water in river networks. Ecosphere 4:17, 1–14

Stager JC, Ryves DB, King C, Madson J, Hazzard M, Neumann FH, Maud R (2013) Late Holocene precipitation variability in the summer rainfall region of South Africa. Quaternary Science Reviews 67:105–120

Sun Q, Xie M, Shi L, Zhang Z, Lin Y, Shang W, Wang K, Li W, Liu J, Chu G (2013) Alkanes, compound-specific carbon isotope measures and climate variation during the last millennium from varved sediments of Lake Xiaolongwan, northeast China. Journal of Paleolimnology 50:331–344

Tanner BR, Uhle ME, Kelley JT, Mora CI (2007) C3/C4 variations in salt-marsh sediments: An application of compound specific isotopic analysis of lipid biomarkers to late Holocene paleoenvironmental research. Organic Geochemistry 38:474–484

Tanner BR, Uhle ME, Mora CI, Kelley JT, Schuneman PJ, Lane CS, Allen ES (2010) Comparison of bulk and compound-specific $\delta^{13}C$ analyses and determination of carbon sources to salt marsh sediments using *n*-alkane distributions (Maine, USA). Estuarine, Coastal and Shelf Science 86:283–291

Tipple BJ, Pagani M (2010) A 35Myr North American leaf-wax compound-specific carbon and hydrogen isotope record: Implications for C4 grasslands and hydrologic cycle dynamics. Earth and Planetary Science Letters 299:250–262

Tissot BP, Welte DH (1984) (eds) Petroleum formation and occurrence, 2nd Ed. Springer-Verlag, New York, NY

Tulipani S, Grice K, Krull E, Greenwood P, Revill AT (2014) Salinity variations in the northern Coorong Lagoon, South Australia: Significant changes in the Ecosystem following human alteration to the natural water regime. Organic Geochemistry 75:74–86

Turner NC, Schulze E-D, Nicolle D, Schumacher J, Kuhlmann I (2008) Annual rainfall does not directly determine the carbon isotope ratio of leaves of Eucalyptus species. Physiologia Plantarum 132:440–445

Unger IM, Motavalli PP, Muzika RM (2009) Changes in soil chemical properties with flooding: A field laboratory approach. Agriculture, Ecosystems & Environment 131:105–110

van der Kaars S, De Deckker P, Gingele FX (2006) A 100 000-year record of annual and seasonal rainfall and temperature for northwestern Australia based on a pollen record obtained offshore. Journal of Quaternary Science 21:879–889

van Etten EJB (2009) Inter-annual Rainfall Variability of Arid Australia: greater than elsewhere? Australian Geographer 40:109–120

van Soelen EE, Wagner-Cremer F, Damste JS, Reichart GJ (2013) Reconstructing tropical cyclone frequency using hydrogen isotope ratios of sedimentary *n*-alkanes in northern Queensland, Australia. Palaeogeography, Palaeoclimatology, Palaeoecology 376:66–72

Verschuren D (1999) Sedimentation controls on the preservation and time resolution of climate-proxy records from shallow fluctuating lakes. Quaternary Science Reviews 18:821–837

Vogts A, Moossen H, Rommerskirchen F, Rullkötter J (2009) Distribution patterns and stable carbon isotopic composition of alkanes and alkan-1-ols from plant waxes of African rain forest and savanna C3 species. Organic Geochemistry 40:1037–1054

Volkman JK, Barrett SM, Blackburn SI, Mansour MP, Sikes EL, Gelin F (1998) Microalgal biomarkers: a review of recent research developments. Organic Geochemistry 29:1163–1179

Volkman JK, Revill AT, Bonham PI, Clementson LA (2007) Sources of organic matter in sediments from the Ord River in tropical northern Australia. Organic Geochemistry 38:1039–1060

Voznesenskaya EV, Akhani H, Koteyeva NK, Chuong SDX, Roalson EH, Kiirats O, Franceschi VR, Edwards GE (2008) Structural, biochemical, and physiological characterization of photosynthesis in two C_4 subspecies of *Tecticornia indica* and the C_3 species *Tecticornia pergranulata* (Chenopodiaceae). Journal of Experimental Botany 59:1715–1734

Weiguo L, Xiahong F, Youfeng N, Qingle Z, Yunning C, Zhisheng AN (2005) $\delta^{13}C$ variation of C3 and C4 plants across an Asian monsoon rainfall gradient in arid northwestern China. Global Change Biology 11:1094–1100

Wolff C, Haug GH, Timmermann A, Damsté JSS, Brauer A, Sigman DM, Cane MA, Verschuren D (2011) Reduced interannual rainfall variability in East Africa during the last ice age. Science 333:743–747

Zhou Y, Grice K, Stuart-Williams H, Farquhar GD, Hocart CH, Lu H, Liu W (2010) Biosynthetic origin of the saw-toothed profile in $\delta^{13}C$ and $\delta^{2}H$ of *n*-alkanes and systematic isotopic differences between *n*-, *iso*-and *anteiso*-alkanes in leaf waxes of land plants. Phytochemistry 71:388–403

Zhou Y, Grice K, Chikaraishi Y, Stuart-Williams H, Farquhar GD, Ohkouchi N (2011) Temperature effect on leaf water deuterium enrichment and isotopic fractionation during leaf lipid

biosynthesis: Results from controlled growth of C_3 and C_4 land plants. Phytochemistry 72:207–213

TABLES

Table 1: Relative abundances of *n*-alkanes (% odd *n*-$C_{27–33}$) and their stable isotopic signatures ($\delta^{13}C$) in leaves from C_3 and C_4 plant taxa found in the semi-arid Pilbara (Arid) and in various climates (All). Sources: Collister et al. 1994; Ficken et al. 2000; Chikaraishi and Naraoka 2003; Bi et al. 2005; Mead et al. 2005; Krull et al. 2006; Rommerskirchen et al. 2006; Tanner et al. 2007; Pedentchouk et al. 2008; Vogts et al. 2009; Diefendorf et al. 2010; Kristen et al. 2010; Tanner et al. 2010; Diefendorf et al. 2011.

		n-C_{27}	std	*n*-C_{29}	std	*n*-C_{31}	std	*n*-C_{33}	std	*n*	mean	std
Arid												
Abundance	C_3	21 ±	14	36 ±	19	30 ±	14	13 ±	15	20	25 ±	15
	C_4	11 ±	7	16 ±	7	45 ±	13	29 ±	15	30	25 ±	10
$\delta^{13}C$	C_3	−32.5 ±	2.1	−33.3 ±	1.8	−34.2 ±	2.2	−35.2 ±	1.9	8–22	−33.8 ±	2.0
	C_4	−22.0 ±	2.6	−21.9 ±	2.0	−22.4 ±	2.2	−22.3 ±	1.8	30–32	−22.2 ±	2.2
All												
Abundance	C_3	15 ±	17	38 ±	24	33 ±	19	14 ±	18	138	25 ±	19
	C_4	14 ±	12	18 ±	12	39 ±	15	29 ±	18	49	25 ±	14
$\delta^{13}C$	C_3	−32.4 ±	2.8	−36.2 ±	2.6	−33.7 ±	3.1	−36.8 ±	2.9	94–176	−34.7 ±	2.9
	C_4	−23.2 ±	5.1	−24.9 ±	5.0	−23.6 ±	5.1	−25.1 ±	5.5	67–88	−24.2 ±	5.2

(2-COLUMN FITTING TABLE)

Table 2: Geochemical parameters of four organic sedimentary periods (P1–P4) from the 14 Mile Pool sediment record, NW Australia.

Parameter		P1 (1990–2012[1])	P2 (1600–1990)	P3 (700–1600)	P4 (<100–700)	Total Av (<100–2012)
Bulk sediment	n (combined intervals)	17	23	7	11	58
content &	Total C (%wt)	1.4	0.6	0.7	<0.4	0.8
stable isotopes	Range	0.8–5.6	<0.4–1.1	0.5–0.9	<0.4–0.5	<0.4–5.6
	Total N (%wt)	0.12	0.03	0.03	0.01	0.05
	Range	0.06–0.17	0.01–0.06	0.02–0.03	<0.01–0.01	<0.01–0.17
	δ^{13}C [‰ VPDB]	−24.3	−22.9	−20.3	−28.2	−23.4
	Range	−26.7–−22.3	−26.2–−20.2	−22.4–−16.9	−28.4–−28.0	−28.4–−16.9
	δ^{15}N [‰ AIR]	6.1	7.5	7.4	7.6	7.1
	Range	4.8–8.4	6.5–7.9	7.0–7.6	7.5–7.8	4.8–8.4
Yield	Tot ext (µg·g^{-1})	155	87	63	< 5	-
	Aliphatic (% tot)	4.7	2.6	5.0	-	-
	Aromatic (% tot)	0.3	8.5	0.7	-	-
	NSO (% tot)	95	89	94	-	-
Aliphatic fraction	Alkanes (%TIC)	84	61	71	-	-
	Steroids (%TIC)	1.4	8.1	7.2	-	-
	Hopanoids (%TIC)	2.7	4.2	5.8	-	-
	Others (% TIC)	12	27	16	-	-
CPI	*n*-$C_{23–33}$	3.1	5.7	5.0	-	-
P_{aq}		0.3	0.1	0.3	-	-
Mixing	C_3 (%)	59	53	50	-	-
	C_4 (%)	41	47	50	-	-

Note: [1]All time periods are provided in years of the Common Era (CE); C and N content (Total C and Total N) and stable carbon and nitrogen isotopes (δ^{13}C and δ^{15}N) (modified from Rouillard et al. 2016); estimated yields of the total extractable fraction (Tot ext; µg·g^{-1} of sediment); the aliphatic, aromatic and polar (NSO) fractions are expressed as a % of the total extractable fraction; relative abundance of *n*-alkanes, steroids, hopanoids and other aliphatic compounds on the total ions chromatogram (%TIC); carbon preference index (CPI) and P_{aq} index (see

(2-COLUMN FITTING TABLE)

LIST OF FIGURES

Figure 1: a–b) Upper Fortescue River catchment delineated (solid black line) on a True-colour Aqua MODIS image (5, Jan 2005; NASA 2005), including b) a vegetation map with Chenopod (Shrublands, Sampire Shrubland and Forblands), Eucalypt (Woodlands; Open Woodlands), Acacia (Shrublands; Open Woodlands; Forests and Woodlands) and Grasslands (Hummock (*Triodia* spp); Tussock); and **c–d)** aerial photographs (flowing East–West, the Upper Fortescue River, the 14 Mile Pool and the Fortescue Marsh) of the **c)** riparian vegetation remaining (green) during dry conditions (Jul, 2010; Photograph: Clive Taylor) and **d)** the greening effect of large rains during the wet season (Feb 2012, one month after Severe Tropical Cyclone Heidi).

(1-COLUMN FITTING IMAGE)

Figure 2: GC-MS total ion chromatograms (TIC) and fragmentograms (*m/z* 191 and 217) of the three periods in the core; (a) P1, (b) P2 and (c) P3. Tentatively assigned compounds are labelled with their corresponding carbon number and unsaturation level (=); odd (C) and even (filled circles) *n*-alkanes, tricyclic terpanes (t), tetracyclic terpanes (T), steroids (s), hopanoids (h) methylated alkane series range (M) and linear aliphatic series (open circles).

(1.5-COLUMN FITTING IMAGE)

Figure 3: Relative peak abundances (% TIC) of the main aliphatic compounds extracted by GC-MS and quantitative distributions of hopanoids and steroids within each sedimentary period.

(1-COLUMN FITTING IMAGE)

Figure 4: Average carbon stable isotopic signature ($\delta^{13}C$) of the *n*-alkanes extracted from each sediment period: P1 (blue), P2 (green) and P3 (orange). Error bars represent the standard deviation obtained from triplicate measurements.

(1-COLUMN FITTING IMAGE)

Figure 5: a) Carbon stable isotopic signatures ($\delta^{13}C$) of long chain *n*-alkanes C_{27}, C_{29}, C_{31} and C_{33} extracted from the P1 to P3 sediments: P1 (dark blue circles), P2 (light green circles) and P3 (orange circles) compared to boxplots showing the range of terrestrial leaf waxes values of C_3 (light and dark green) and C_4 (light and dark yellow) plants as described in the literature (wide light coloured boxes) and the arid zone subset (thin dark coloured boxes); **b)** change in end-members contribution over time, i.e., probability distributions of contribution from C_3 (dark green) and C_4 (yeallow) sources (SIAR).

(1-COLUMN FITTING IMAGE)

Figure 6: Relationship between foliar $\delta^{13}C$ and mean annual precipitation of woody (C_3) riparian (filled blue circles) and non-riparian (filled orange triangles) vegetation from the Pilbara (collected between 1997 and 2013 by the Ecosystem Research Group at The University of Western Australia; see Table S2 for more information of species and sampling of the Pilbara dataset) compared to the global distribution (open grey circles; modified from Diefendorf et al. 2010).

(1-COLUMN FITTING IMAGE)

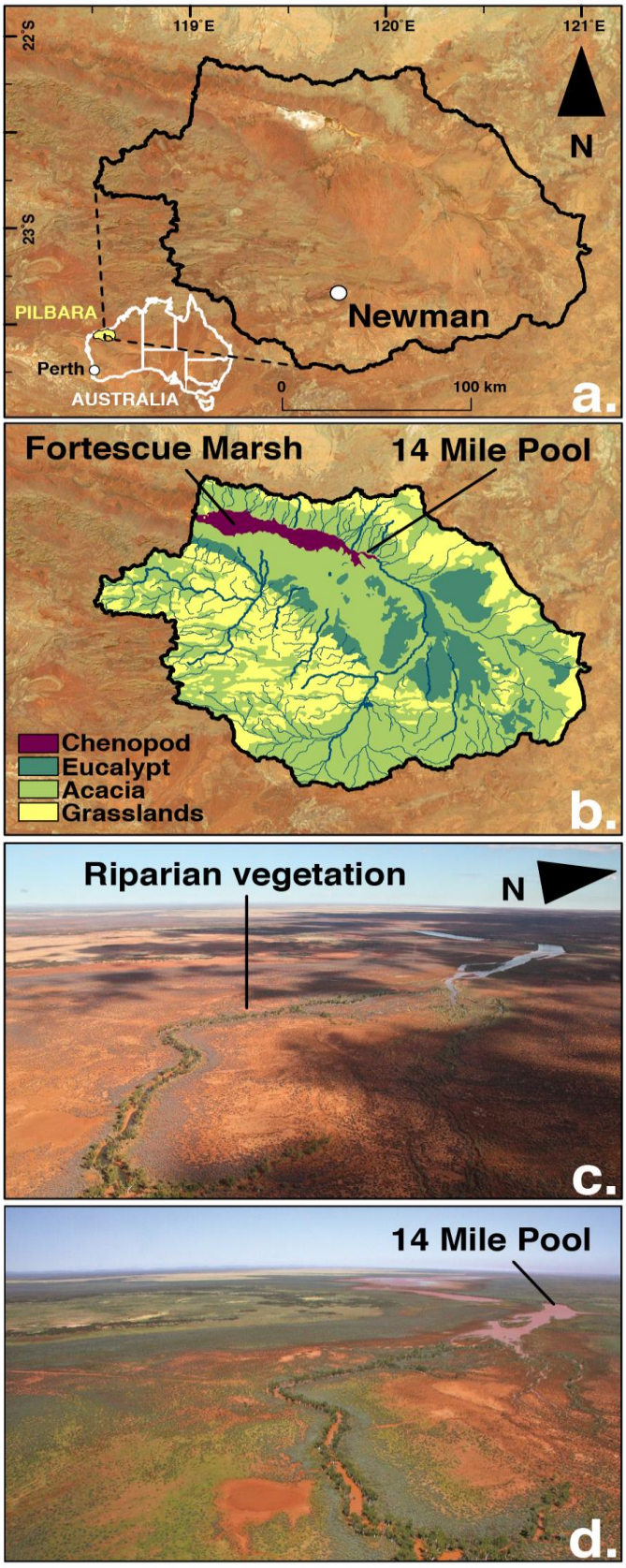

Fig. 1

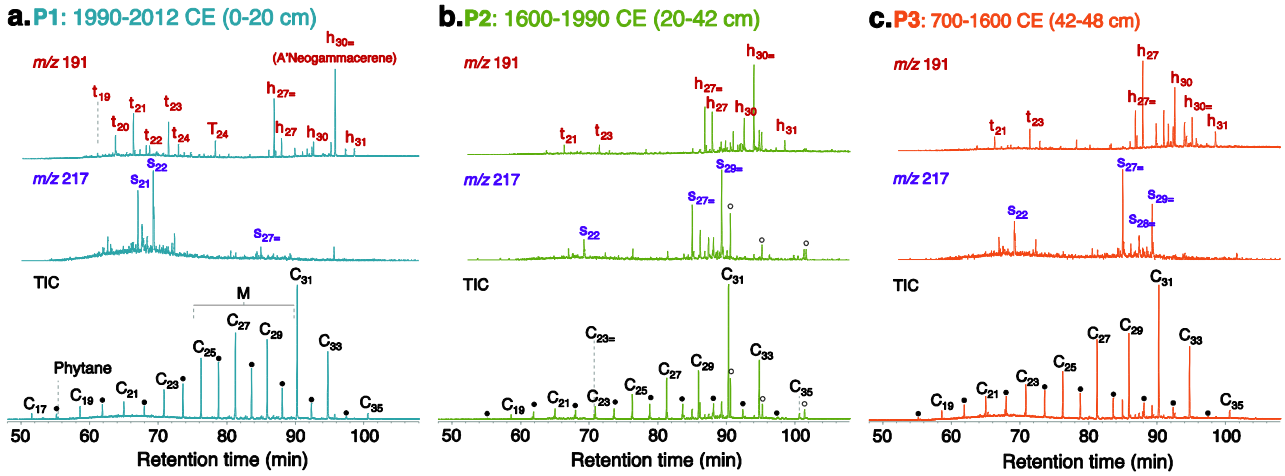

Fig. 2

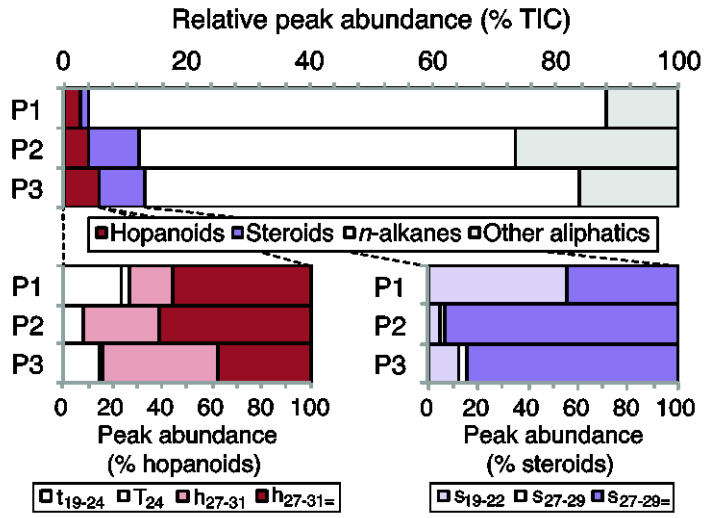

Fig. 3

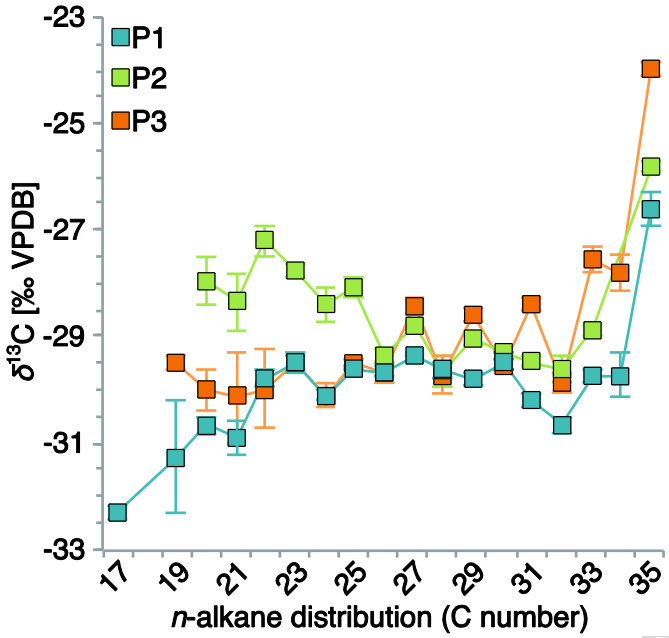

Fig. 4

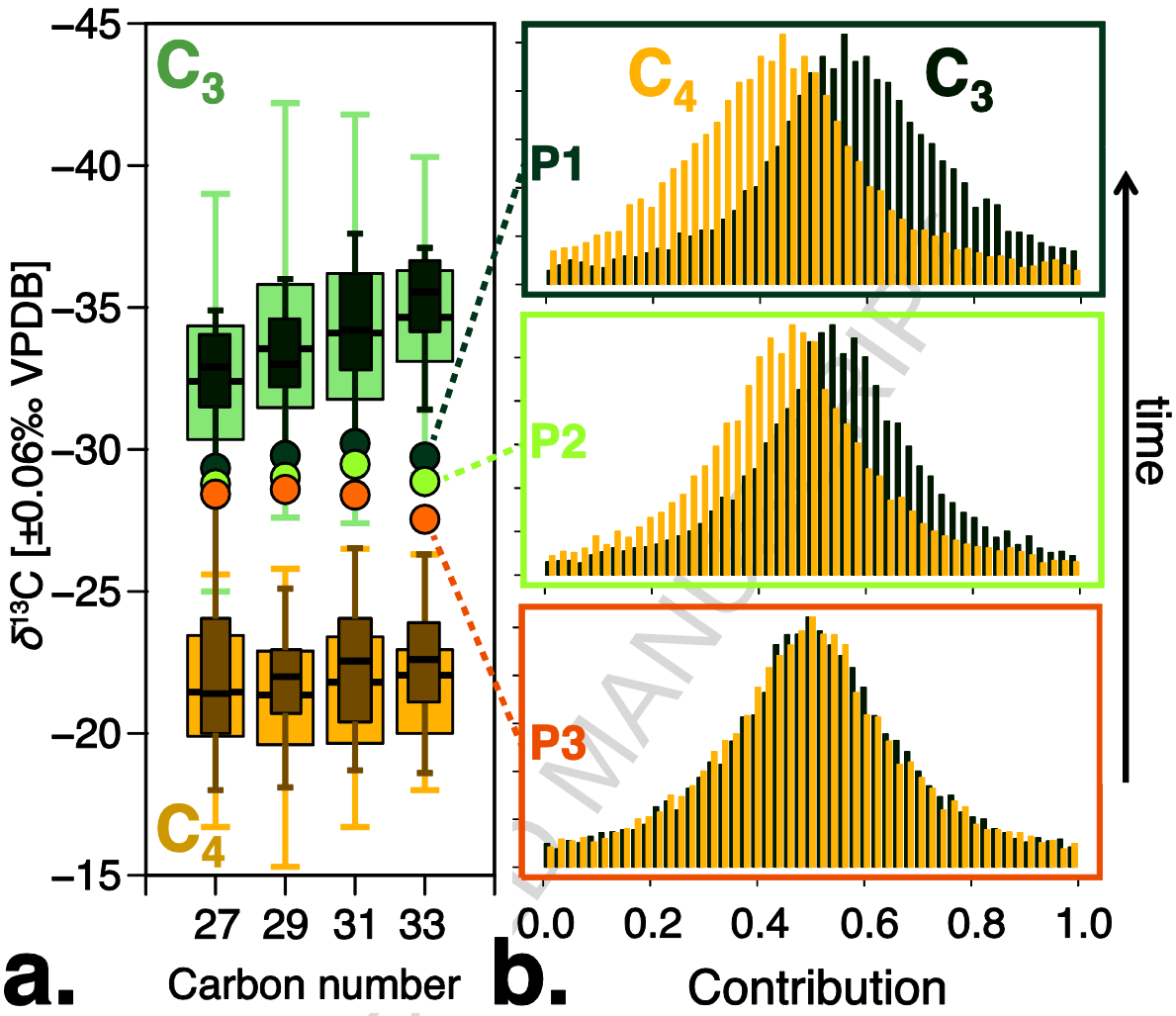

Fig. 5

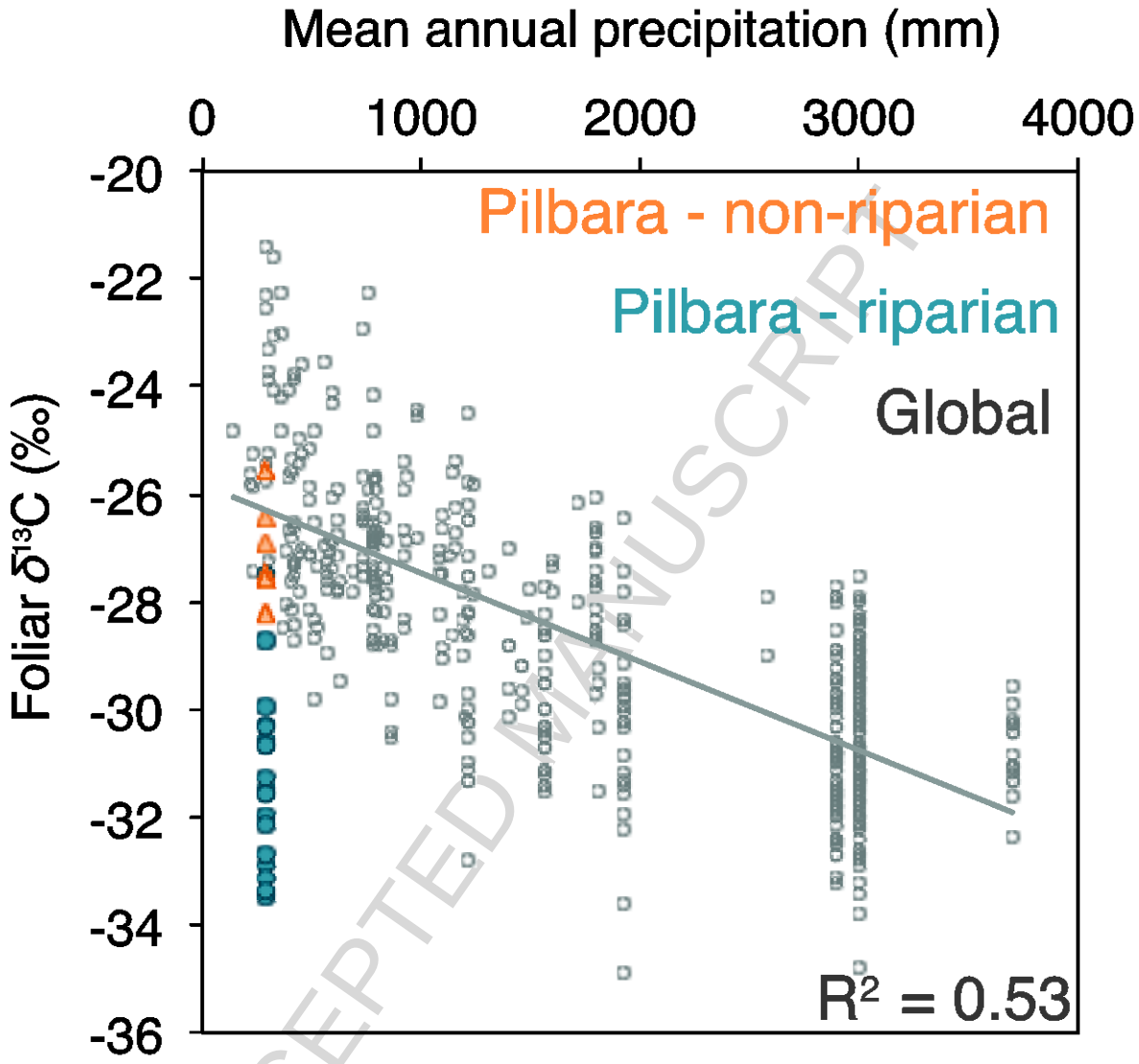

Fig. 6

HIGHLIGHTS

- Biomarkers and *n*-alkane $\delta^{13}C$ were extracted from sediment with total C = 0.4–1.4%
- Distribution of biomarkers reflected a decrease of aridity in the last ~2000 years
- Arid based Bayesian model of *n*-alkanes $\delta^{13}C$ suggested increase of riparian C_3 input
- Provided interpretive framework for reconstructions in tropical arid ecosystems